DRAFT MANUSCRIPT

AIR QUALITY SIMULATIONS OF WILDFIRES IN THE PACIFIC NORTHWEST EVALUATED WITH SURFACE AND SATELLITE OBSERVATIONS DURING THE SUMMERS OF 2007 AND 2008

Farren L. Herron-Thorpe[1], George H. Mount[1], Louisa K. Emmons[2], Brian K. Lamb[1], Dan A. Jaffe[3,4], Nicole L. Wigder[3,4], Serena H. Chung[1], Rui Zhang[1], Matthew D. Woelfle[3], & Joseph K. Vaughan[1]

[1] Laboratory for Atmospheric Research; Washington State University, Pullman, WA, USA

[2] National Center for Atmospheric Research; Boulder, CO, USA

[3] Department of Atmospheric Sciences; University of Washington, Seattle, WA, USA

[4] School of Science, Technology, Engineering and Mathematics; University of Washington-Bothell, Bothell, WA, USA

Abstract

Evaluation of a regional air quality forecasting system for the Pacific Northwest was carried out using a suite of surface and satellite observations. Wildfire events for the 2007 and 2008 fire seasons were simulated using the Air Information Report for Public Access and Community Tracking v.3 (AIRPACT-3) framework utilizing the Community Multi-scale Air Quality (CMAQ) model. Fire emissions were simulated using the BlueSky framework with fire locations determined by the Satellite Mapping Automated Reanalysis Tool for Fire Incident Reconciliation (SMARTFIRE). Plume rise was simulated using two different methods: the Fire Emission Production Simulator (FEPS) and the Sparse Matrix Operator Kernel Emissions (SMOKE) model. Predicted plume top heights were compared to the Cloud-Aerosol LIDAR with Orthogonal Polarization (CALIOP) instrument aboard the Cloud Aerosol LIDAR and Infrared Pathfinder Satellite Observation (CALIPSO) satellite. Carbon monoxide predictions were compared to the Atmospheric InfraRed Sounder (AIRS) instrument aboard the Aqua satellite. Horizontal distributions of column aerosol optical depth (AOD) were compared to retrievals by the Moderate Resolution Imaging Spectroradiometer (MODIS) instrument aboard the Aqua satellite. Model tropospheric nitrogen dioxide distributions were compared to retrievals from the Ozone Monitoring Instrument (OMI) aboard the Aura satellite. Surface ozone and PM2.5 predictions were compared to surface observations. The AIRPACT-3 model captured the location and transport direction of fire events well, but sometimes missed the timing of

fire events and overall underestimated the PM2.5 impact of wildfire events at surface monitor locations. During the 2007 (2008) fire period the fractional biases (FB) of AIRPACT-3 for various pollutant observations included: average 24-hr PM2.5 FB=-33% (-27%); maximum daily average 8-hr ozone FB= -8% (+1%); AOD FB= -61% (-53%); total column CO FB= -10% (-5%); and tropospheric column NO_2 FB= -39% (-28%). The bias in total column CO is within the range of expected error. Fractional biases of AIRPACT-3 plume tops were found to be -46% when compared in terms of above mean sea level (AMSL), but only -28% when compared in terms of above ground level (AGL), partly due to the under-estimation of AIRPACT-3 ground height in complex terrain that results from the 12-km grid-cell smoothing. We conclude that aerosol predictions were too low for locations greater than ~100-300 km downwind from wildfire sources and that model predictions are likely under-predicting secondary organic aerosol (SOA) production due to a combination of very low VOC emission factors used in the United States Forest Service Consume model, an incomplete speciation of VOC to SOA precursors in SMOKE, and under-prediction by the SOA parameterization within CMAQ.

1 Introduction

1.1 MOTIVATION

The Pacific Northwest is home to a rural landscape that periodically

64 experience large wildfires, especially during dry summers. Wildfire smoke
65 and other particulate matter (PM) emitted into the atmosphere can cause
66 severe health problems. Informing the public about upcoming poor air
67 quality expected from fires requires a comprehensive knowledge of fire
68 locations, land type being burned, terrain, wind direction, available moisture,
69 timing, and other conditions. Reports generated by fire fighters are quickly
70 provided to air quality managers by the United States Forest Service, but it is
71 difficult to get an accurate assessment of wildfire conditions in remote
72 locations with rough terrain, few access roads, and sparse air quality monitor
73 distribution. Meteorological forecasts and chemistry transport models can be
74 used to predict the air quality impacts of wildfire emissions, but the task is
75 challenging (Simon et al., 2012). Satellite retrievals of air quality indicators
76 provide a valuable asset that, when combined with surface measurements,
77 can help to assess the validity of air quality models simulating large wildfire
78 events. The analysis presented here utilizes multiple satellite products to
79 evaluate simulations from the Air Information Report for Public Access and
80 Community Tracking v.3 (AIRPACT-3) regional air quality model, which
81 utilizes the BlueSky fire emissions framework and the Community Multi-scale
82 Air Quality (CMAQ) model. As such, this work demonstrates how a suite of
83 satellite products can be combined with in-situ observations to inform
84 improvement of air quality forecast performance.

85 The objective of this work is to report the level of performance and
86 types of error that were found for modeled fire locations, plume heights, and

pollutant concentrations simulated in AIRPACT-3 based on a combination of satellite products and surface pollutant observations. It is essential that future AIRPACT versions accurately predict the impact of fires, given the very large fire seasons in recent history (e.g. 2012) and the expected increase of fire activity as the regional climate changes. We chose to use finalized activity reports to derive wildfire emissions, rather than forecast-mode data, so that we could focus on the emissions from known fire events and test the model's performance in a "best-case" scenario. We modeled wildfire events that occurred during the summers of 2007 and 2008 because of their interest to AIRPACT users, the extensive fire activity that occurred, and because satellite coverage throughout NASA's Afternoon Train (A-Train) of satellites was relatively complete. We focused on A-Train satellite data to keep overpass times consistent (~1:45 PDT) and because fire activity is best detected in the afternoon, when wildfires are most active. Simulations of the historically large fires that ignited in Idaho, Nevada, and Montana throughout July of 2007 provided great insight into AIRPACT-3 wildfire performance. In addition, the Northern California fires that ignited June 21, 2008 provided further valuable model information due to the technical challenge posed by the large fires that occurred on both sides of the southern boundary of the modeling domain.

1.2 FIRE ACTIVITY OF 2007 AND 2008

The western US experienced abnormally dry winter and spring seasons in 2007, which led to a summer drought and extensive wildfire events in

110 Idaho, Nevada, and Montana. Extreme temperatures and sparse
111 precipitation during early summer 2007, coupled with lightning activity and
112 several strong wind events, led to several expanding, long-lived fires.
113 Precipitation events that started on August 17 slowed the expansion of
114 wildfires and allowed fire fighters to contain many of the burning areas,
115 though some fires continued to burn into September. The National
116 Interagency Coordination Center (NICC) at the National Interagency Fire
117 Center (NIFC; http://www.predictiveservices.nifc.gov/) reported that over
118 800,000 acres burned in Nevada during July 2007. By August 31 the Great
119 Basin and Northern Rockies had wildfires that burned over 4 million acres,
120 nearly twice the typical year-to-date area burned, with eight large fires or
121 complexes having burned more than 100,000 acres each.

122 The summer of 2008 was also dry but experienced significantly less
123 fire activity across the US, except for California and parts of the southern
124 U.S. Northern California, part of which is in the AIRPACT-3 domain, reported
125 over 850,000 acres burned, which was nearly 9 times the 10-year average
126 for that region. On June 20 - 21, 2008, widespread lightning started nearly
127 one thousand fires in northern California and those in remote and difficult
128 terrain burned for many days. Lightning storms in mid-August 2008 also
129 caused numerous large fires in Idaho and Montana. The number of acres
130 burned by state reported by the NICC NIFC is shown in Table 1 for 2007 and
131 2008. Analysis of O_3 and particulate matter enhancements at the Mt
132 Bachelor Observatory by Wigder et al. (2013) identified 14 individual fire

plumes in 2008 and 6 in 2007.

The analysis presented here includes results for two separate time periods: July 3 – August 22, 2007 and June 22 – August 27, 2008, which were chosen to include the largest annual fire events in the AIRPACT-3 domain. Details about each reported fire complex that burned during the analysis period are given in Table S1 of the Supplementary Materials. Fire events during the analysis periods that included at least one reported fire over 5,000 acres of burn area are shown in Fig. 1 (Fig. S1 includes labels for fire complex names).

2 Methods

2.1 AIRPACT-3 AIR QUALITY MODELING SYSTEM

The AIRPACT-3 modeling system (Chen et al., 2008; Herron-Thorpe et al., 2010, 2012) simulates air quality in the Pacific Northwest with the CMAQ v4.6 chemical transport model (Byun and Schere, 2006). Area and non-road mobile emissions are from the 2002 EPA NEI, projected to 2005 using the EPA's Economic Growth Analysis System (EGAS) software; on-road mobile emissions are based on the EPA MOBILE v6.2; anthropogenic emissions for Canada are from the 2000 Greater Vancouver Regional District (GVRD) inventory; and biogenic emissions are obtained from the Biogenic Emissions Inventory System version 3 (BEIS-3). The AIRPACT-3 base emissions are spatially and temporally allocated using the Sparse Matrix Operator Kernel Emissions (SMOKE) v2.4 model while all fire emissions are processed with

155 the SMOKE v2.7 model. The AIRPACT-3 domain includes a 95 x 95 grid of 12
156 km x 12 km cells using 21 layers from the surface to the lower stratosphere.
157 The version of CMAQ used includes the SAPRC-99 chemical kinetic
158 mechanism, the ISOROPIA inorganic aerosol equilibrium module, and the
159 Secondary Organic Aerosols Model (SORGAM). Meteorology inputs for
160 AIRPACT-3 were derived from forecasts by Mass and colleagues
161 (http://www.atmos.washington.edu/mm5rt/; Mass et al., 2003) and
162 preprocessed for CMAQ using the Meteorology Chemistry Interface Processor
163 (MCIP). The Mesoscale Model v5 (MM5; Mass et al., 2003) was used for the
164 year 2007 simulations while the Weather Research and Forecasting (WRF;
165 Skamarock et al., 2005) model was used for the year 2008 simulations.
166 Model of OZone And Related Tracers, version 4 (MOZART-4; Emmons et al.,
167 2010) simulations produced at the National Center for Atmospheric Research
168 (NCAR) were used as chemical boundary conditions around the AIRPACT-3
169 domain (Emmons et al., 2010; Herron-Thorpe et al., 2012). The MOZART-4
170 simulations included the assimilation of satellite CO column v4 retrievals from
171 the Measurement Of Pollution In The Troposphere (MOPITT) instrument, a
172 gas-correlation radiometer on-board the NASA Terra satellite (Deeter et al.,
173 2010). The MOZART-4 emissions are the same as those used in Wespes et
174 al. (2012), which include anthropogenic emissions based on the inventory
175 developed by D. Streets for the NASA ARCTAS experiment
176 (http://bio.cgrer.uiowa.edu/arctas/emission.html) and biomass burning
177 emissions from FINN (Fire Inventory from NCAR, Wiedinmyer et al., 2011).

178 Fire location, area, and emissions were calculated using BlueSky v3.1
179 data (http://www.airfire.org/bluesky), which utilizes United States Forest
180 Service fire reports and hotspot detects reported by the Hazard Mapping
181 System (HMS) together in the Satellite Mapping Automated Reanalysis Tool
182 for Fire Incident Reconciliation (SMARTFIRE; Larkin et al., 2009 and Raffuse
183 et al., 2009). SMARTFIRE reports wildfire locations (Larkin et al., 2009;
184 Strand et al., 2012), but is ultimately limited by the accuracy and
185 completeness of the satellite detects and USFS reports filed. Air quality
186 forecasts use the fire locations reported over the past 48-hours and assume
187 them to persist throughout the simulation. However, the fire reports used in
188 this model reanalysis are from the final SMARTFIRE archive, as distinct from
189 the information reported in near real-time, which allows us to scrutinize the
190 model performance independent of the near real-time fire reporting system.

191 For this analysis, the BlueSky framework (Larkin et al., 2009; Raffuse
192 et al., 2009) was operated in default mode, which includes the use of the
193 Consume v3 (Ottmar et al., 2009), Fuel Characteristic Classification System
194 v1 (FCCS; Riccardi et al., 2007), and Fire Emission Production Simulator v1
195 (FEPS; Anderson et al., 2004) software programs provided by the USFS.
196 FCCS v1 provides vegetation type and corresponding fuels (Fig. 1) at 1-km
197 resolution based on Bailey ecoregions and satellite-derived cover type, which
198 provides input to Consume. Consume was developed empirically using a
199 variety of vegetation types and fire conditions, providing fuel consumption
200 and emissions by combustion phase (smoldering or flaming) data to FEPS.

FEPS calculates the heat released and the individual pollutant emissions, based on combustion efficiency of the burn. The default behavior of BlueSky classifies fuels as "dry", unless otherwise reported by SMARTFIRE. This can result in large over-predictions during events that don't consume most available fuels, but generally it is reasonable to assume that fire activity occur in areas with dry fuels. A summary of the fire-related model pathways used for AIRPACT-3 is shown in Fig. 2.

Two plume rise methods were used in this analysis, resulting in two sets of AIRPACT-3 model results. The first method uses the SMOKE-ready files created by BlueSky, which include hourly information, to explicitly set the plume rise to what FEPS predicts. The second set of model simulations were performed using methods that bypassed the FEPS plume rise algorithm and instead converted standard BlueSky output to create daily input files for SMOKE. It is important to note that the two plume rise methods used are based upon the same heat flux and smoldering/flaming emissions ratios but results differ in two ways: 1) whereas FEPS plume rise method allocates all smoldering emissions to the surface layer, the SMOKE plume rise method allows for smoldering emissions to be allocated throughout multiple layers near the surface; and 2) whereas FEPS plume rise method does not utilize meteorology or surface elevation when predicting flaming plume heights, the SMOKE plume rise method computes flaming plume heights as a function of buoyancy using the heat content predicted by BlueSky, modeled meteorology, and modeled terrain heights (Pouliot et al., 2005).

2.2 AQUA-MODIS AOD

The Aqua satellite was launched in May 2002 carrying the Moderate Resolution Imaging Spectroradiometer (MODIS) as part of NASA's Afternoon-Train (A-Train) of Earth Observing Satellites (EOS). The Aqua-MODIS retrievals provide aerosol information at nearly the same time as the other A-Train instruments, allowing coincident multi-species analyses, as presented in this analysis. Aqua MODIS reliably retrieves Aerosol Optical Depth (AOD; τ) for much of the globe on a daily basis with a nadir footprint of 10 km. Algorithms described by Remer et al. (2005) are used to interpolate the 470 nm and 660 nm retrievals to provide a 550-nm AOD product (MYD04_L2 v5.1; Land_and_Ocean) where only the highest quality data (Quality Flag=3) is used. Typical AOD values at a clean site are below 0.3, while values over 1.0 are indicative of multiple scattering caused by high aerosol loading (i.e. heavy haze, biomass burning, or dust events). The maximum AOD values historically retrieved by MODIS are ~5.0, but these are rare events. MODIS AOD error is not reported for each pixel but studies have validated the an error of 15%, which is influenced by unique aerosol composition, varied land cover color, cloud fringes, and snow cover at high elevations (Levy et al., 2007 and Drury et al., 2008). MODIS AOD retrievals are useful in areas with no clouds but they have been shown to be biased low compared to AERONET and MISR (Kahn et. al, 2010 and Eck et. al, 2013).

All MODIS AOD retrievals used in this analysis were projected to the AIRPACT-3 grid by using the pixel with the closest proximity to the center of

each AIRPACT-3 grid-cell. This method gives a more detailed map than would otherwise be calculated using weighted spatial interpolation, and is suitable here since the MODIS spatial resolution is finer than AIRPACT-3. AIRPACT-3-simulated aerosol distributions were generated for all modeled aerosol species: nitrates, sulfates, ammonium, elemental carbon (EC), organic particulates, and coarse mode aerosols. AOD was calculated from AIRPACT-3 simulated aerosol species concentrations and size distributions using algorithms developed by Binkowski and Roselle (2003). This method uses the simulated aerosol total volume concentration for the Aitken and accumulation mode aerosols and their associated Mie extinction efficiencies to calculate AOD per modeled layer, which is then integrated vertically through the troposphere to yield the reported model AOD. An accurate approximation method from Evans and Fournier (1990) was used to calculate the Mie extinction efficiency factors. AIRPACT-3 grid-cells that did not have corresponding high-quality MODIS retrievals were omitted from the analysis.

2.3 AIRS CO

In addition to MODIS, the Aqua satellite includes the Atmospheric Infra-Red Sounder (AIRS), which provides information about weather and trace gases. The AIRS instruments are an infrared spectrometer and a visible light/near-infrared photometer. The AIRS total column carbon monoxide level-2 v5 product used in this analysis (AIRX2RET) provides data reported on the Advanced Microwave Sounding Unit (AMSU) ground footprint, which varies from 36 km x 36 km to 50 km x 50 km. AIRS level-2

v5 data includes 7 trapezoidal layers of CO mixing ratio in the troposphere and an averaging kernel matrix for the full 9-layer profile available in the support product files. In this study the AIRPACT-3 profiles were convolved with the AIRS averaging kernels as discussed in Olsen et al. (2007) and Maddy and Barnet (2008), and the total column CO values were then interpolated to the original AIRPACT-3 projection using a Delaunay triangulation scheme. The AIRS averaging kernel slightly reduces the AIRPACT-3 total column CO, with some loss of information in the lower troposphere and enhanced middle troposphere sensitivity (Herron-Thorpe et al., 2012). AIRS typically has only 1 degree of freedom in the troposphere, with its greatest sensitivity to the mid-troposphere. Thus AIRS retrievals likely underestimate total column CO for fire plumes contained within a shallow boundary layer. However, the convolution of the model with the AIRS averaging kernels should address potential comparison problems. The typical reported error in the AIRS CO product varies by layer, with moderate error (~45%) throughout the middle and upper troposphere and even larger error (~60%) in the lower troposphere. However, large CO values (e.g. greater than 2.3E+18 molec./cm^2), as the case with large fire plumes, are typically associated with very low errors (10-20%) throughout the layers.

2.4 OMI TROPOSPHERIC NO_2

The Aura satellite successfully joined the A-Train in July 2004, carrying multiple instruments that retrieve information about atmospheric chemistry. Although tropospheric ozone retrieved by the Ozone Monitoring Instrument

(OMI) is typically not precise enough for this wildfire analysis, the tropospheric NO_2 columns provided by the Tropospheric Emission Monitoring Internet Service (TEMIS; http://www.temis.nl/airpollution/no2.html) are of significant value. The Derivation of OMI tropospheric NO_2 (DOMINO) algorithms calculate air mass factors (AMF), a priori profiles, stratospheric NO_2, and ghost columns from the daily global Tracer Model v4 (TM4), which is driven with meteorological fields from the European Centre of Medium-Range Forecasts (ECMWF) (Boersma et al., 2011). The product provides tropospheric NO_2 column retrievals with a 13 km x 24 km footprint at nadir with increasing footprint size as the observation moves off-nadir. A pixel's "ghost column" (below cloud) is estimated from the a priori profile for the pixel and OMI's retrieval of NO_2 above the cloud cover pressure level, with vertical sensitivity defined by the averaging kernel. The sum of the OMI ghost column and tropospheric column can be compared to a model column for an estimate of model performance. However, when the model NO_2 profile is convolved with the averaging kernel, the ghost column is no longer required. Typical reported errors in the DOMINO product are lowest (~25%) where there is a large signal (e.g. over 2E+15 molec/cm^2) but errors are typically much higher (~50%) when the signal is considerably less.

Since OMI's NO_2 averaging kernel shows decreasing sensitivity as the vertical profile approaches the surface, the result of applying the averaging kernel to AIRPACT-3 NO_2 allows for essentially a "free troposphere" comparison with OMI. In this study we used OMI pixels with low cloud

316 fraction (<35%) and convolved all AIRPACT-3 profiles with the OMI
317 averaging kernel. AIRPACT-3 cells that fall within the spatial boundaries of
318 each OMI pixel were averaged and interpolated, effectively reducing the
319 resolution of the model results to equal that of the co-located OMI pixel, and
320 then both were interpolated to the original AIRPACT-3 projection using a
321 Delaunay triangulation scheme. This method works well for most areas but
322 can lead to inconsistencies over areas with complex terrain (Herron-Thorpe
323 et al., 2010). Comparisons of CMAQ NO_2 to satellite retrievals also have
324 inherent uncertainty associated with the rapid conversion of NOx to PAN and
325 nitrate (Alvarado et al., 2010 and Akagi et al., 2012).

326 *2.5 CALIOP AEROSOL DETECTION*

327 The Cloud Aerosol LIDAR and Infrared Pathfinder Satellite Observation
328 (CALIPSO) satellite successfully joined the A-Train in April 2006, carrying the
329 Cloud-Aerosol LIDAR with Orthogonal Polarization (CALIOP) instrument as its
330 main payload. CALIOP transmits a linearly polarized laser pulse and then
331 detects the light that is reflected back. Determining the aerosol type from
332 this space-based LIDAR depends on the attenuated backscatter, altitude,
333 location, surface type, and the volume depolarization (ratio of the
334 perpendicular backscatter to the parallel backscatter of the laser light
335 retrieved). Detailed information about the CALIOP data is in the CALIPSO
336 Users Guide (http://www-
337 calipso.larc.nasa.gov/resources/calipso_users_guide/). The laser beam
338 diameter of CALIOP is ~90 meters at the Earth's surface, combined with a

horizontal resolution along scan that varies from 333 m (surface) to 1 km (8.5 km to 20 km altitude). The v3.01 CALIOP level-2 Vertical Feature Mask (Liu et al., 2005; Mielonen et al., 2009; and Winker et al., 2009) product available from the NASA Langley Research Center Atmospheric Science Data Center was used to evaluate AIRPACT-3 plume top height performance. We evaluated plume top heights above mean sea level (AMSL) and above ground level (AGL), so that discrepancies in terrain height could be evaluated. For this analysis, we consider AGL plume heights to be relative to the ground level reported by the respective dataset.

2.6 DAILY REMOTE SENSING ACTIVITY

In addition to the methods described above, we also assessed overall fire conditions using MODIS true-color imagery of smoke plumes with markers for hot-spot locations, available from the Land Atmosphere Near Real-time Capability for EOS (LANCE; USA subset 1; http://lance-modis.eosdis.nasa.gov/imagery/subsets/index.php?project=fas). A daily remote sensing log of the LANCE-MODIS imagery and corresponding remote sensing comparisons, derived from the AIRPACT-3 FEPS plume-rise scenario, was also compiled (Tables S2 – S5). Each fire region that was significantly over the signal-to-noise threshold was counted and tallied in the daily remote-sensing log for AOD and tropospheric NO_2 comparisons. AIRS resolution did not allow us to identify "distinguishable events" and were not tallied. The horizontal footprint and sensitivity of each remote sensing instrument varies, thus distinguishable events counted in the log ranged

from strong isolated fires to large areas with numerous mixed plumes.

2.7 MODEL PERFORMANCE STATISTICS AND GROUND-SITE SELECTION

Definitions of the model performance statistics used are shown in Table 2. Guidance on the treatment of negative values in satellite products suggests that long-term studies (e.g. with time-averaging) should retain the negative values so that no artificial bias is introduced for clean conditions (see http://modis-atmos.gsfc.nasa.gov/MOD04_L2/format.html). However, we were interested in short-term pollution events and chose to discard negative OMI and MODIS values. This approach helped us avoid spurious fractional statistics because it allowed little signal from the variance in "unpolluted" satellite retrievals and focused our statistics on "polluted" events. To assess the model performance for wildfire impacts, the ground-site analysis presented here uses combinations of 140 U.S. surface monitor locations where AIRPACT-3 predicted more than double the normal surface PM2.5 levels sometime during the analysis as an indicator of wildfire impacts. Surface monitor datasets that were excluded from the analysis had one or more of the following problems: no quality-controlled hourly dataset was available, the site was primarily indicative of urban emissions, the site was in Canada (AIRPACT-3 has no wildfire emissions in the Canadian part of the domain), or the site exhibited no distinguishable increase in surface PM2.5 during fire events. The 2007 analysis period had 67 qualified PM2.5 sites and 10 qualified ozone sites; while the 2008 analysis period had 82 qualified PM2.5 sites and 18 qualified ozone sites. The primary analysis of AOD,

385 tropospheric column NO_2, and total column CO includes all 140 site locations.
386 For the purpose of generating model performance statistics, we assessed
387 model performance at these discrete site locations rather than across the
388 entire domain. This was done so that surface monitor observations and
389 satellite retrievals could be compared more consistently, and so that the
390 randomness of the location of usable retrievals did not skew our results
391 spatially or with urban signatures. A more selective rural-sites-only subset
392 includes 43 locations with no possible influence of transported urban pollution
393 in the remote sensing records. This rural-sites-only subset is used for the
394 "matched-threshold" analysis to help determine model performance for fire-
395 polluted cases by only including instances where AIRPACT-3 and the
396 monitor/retrieval in question both surpassed a threshold value: 10 $\mu g/m^3$ for
397 the average 24-hr surface PM2.5, 0.3 for AOD, 1.0E+15 molecules/cm^2 for
398 tropospheric column NO_2, and 1.9E+18 molecules/cm^2 for total column CO.

399 All surface monitor comparisons in this analysis (Fig. S2) were made
400 using hourly data from the EPA Air Quality System
401 (http://www.epa.gov/ttn/airs/airsaqs/detaildata/downloadaqsdata.htm),
402 except for data from Mt. Bachelor Observatory (MBO) in the Oregon Cascade
403 mountains, which is not an AQS reporting site. The Mt. Bachelor Observatory
404 has been used to collect air quality data since 2004, including near-
405 continuous observations of CO, O_3, aerosol scattering and meteorological
406 parameters, and various other chemical species during intensive campaigns.
407 MBO is located at coordinates 43.98° N, 121.69° W at an elevation of 2.7

408 km. The site has been used to investigate long-range transport of Asian
409 pollution and biomass burning, regional wildfires, and other events including
410 stratospheric intrusions (Weiss-Penzias et al., 2006; Ambrose et al., 2011;
411 Wigder et al., 2013). AIRPACT-3 $PM_{2.5}$ and carbon monoxide concentrations
412 were extracted from the layer corresponding to a height of 2.7 km AMSL in
413 the model for comparisons to Mt. Bachelor Observatory to account for the
414 discrepancy in model surface height.

415 **3 Results**

416 *3.1 AIRPACT-3 compared to AIRS, MODIS, and OMI*

417 Remote sensing of atmospheric gases and aerosols is limited by cloud
418 conditions and the source signal strength at the relevant infrared/visible/UV
419 wavelengths. Maps of AOD, tropospheric NO_2 column, and total carbon
420 monoxide column for analysis days in 2007 (2008) with favorable remote-
421 sensing conditions are shown in Figs. 3, 4 (5, 6) for the SMOKE plume-rise
422 scenario (see Figs. S3-S8 for the FEPS plume-rise scenario).

423 On July 22, 2007, AIRPACT-3 under-predicted AOD related to fires in
424 Montana, southern Idaho, and Nevada (Figs. 3, S3). AIRPACT-3 also under-
425 predicted tropospheric column NO_2 in Nevada and Montana on July 22, 2007
426 but the largest modeled fires were not observed via remote sensing, in
427 central Idaho near the Montana border, likely due to mismatch in timings of
428 fire emissions and satellite detections. August 12, (Figs. 4, S4) and August
429 18 (Figs. S5a, S5b) show typical AIRPACT-3 comparisons during the largest

fire periods in 2007. AIRPACT-3 under-estimated the fire-generated pollutants from N. California on June 29, 2008 (Figs. 5, S6) and missed pollutants transported from outside of the domain. AIRPACT-3 did better predicting fires in N. California on July 11, 2008 (Figs. S7a, S7b) but continued to miss fire-generated pollutants from outside of the domain. This is especially evident in Nevada when fire-generated AOD originating from south of the AIRPACT-3 domain is observed but not predicted, suggesting that boundary conditions derived from the MOZART-4 simulations under-predict the influence of fires from outside the domain. AIRPACT-3 did well predicting an interesting transport case on July 20, 2008 but over-predicted the near-source pollutants in N. California/S. Oregon while under-predicting the transported aerosol from within the domain and over-predicting the transported CO from within the domain (Figs. 6, S8). In general, fire locations and air quality impacts were predicted well near fire sources, but AOD predictions were often too low in regions beyond 100 km downwind of large fires. Furthermore, AIRPACT-3 did not predict the observed fire impacts in Nevada that were transported from south of the domain.

The Daily AOD Log for 2007 (2008) discussed in Table S2 (S4) notes that there were 44 (64) days in the period analyzed that confidently showed MODIS AOD due to fires: of the 176 (108) total discernible events, 8% (6%) were observed but not predicted, 37% (32%) were under-predicted, 30% (31%) were predicted well, 20% (18%) were over-predicted, and 5% (13%) were predicted but not observed. We found that the magnitude of predicted

AOD that extended to large distances from sources inside the domain was under-predicted for 13% (31%) of discernible events. Additionally, we found that the magnitude of predicted AOD from sources outside the domain was under-predicted during 8 (27) of the 44 (64) days. There were also 2 (3) days where MODIS AOD clearly showed aerosol loading retained from the previous day that were not predicted. The Daily NO_2 Log for 2007 (2008) in Table S3 (S5) also notes that there were 31 (44) days in the period analyzed that confidently showed tropospheric NO_2 due to fires: of the 122 (76) total discernible events, 0% (4%) were observed but not predicted, 23% (13%) were under-predicted, 21% (30%) were predicted well, 48% (37%) were over-predicted, and 8% (16%) were predicted but not observed. There was also one day (July 1, 2008) where OMI clearly showed tropospheric NO_2 loading retained from the previous day that was not predicted.

Overall, AIRPACT was biased low for all analyzed pollutants for both the 2007 and 2008 timelines. In comparison, for non-fire periods across the whole domain, AIRPACT tends to over-estimate long-term average PM2.5 levels by ~3% (Chen et al., 2008). The 2007 (2008) fractional biases of the SMOKE plume rise scenario for all 140 sites were -61% (-53%) for AOD, -39% (-28%) for tropospheric column NO_2, and -10% (-5%) for total column CO. The FEPS plume rise scenario changed results by a few percent with fractional biases of -66% (-58%), -38% (-26%), and -13% (-7%), respectively (Table 3). In comparison, the fractional biases for the matched-threshold analysis of the SMOKE plume rise scenario for all 43 rural sites

476 (where both the model and satellite retrieval were greater than 0.3 AOD,
477 1.9E+18 VCD CO, or 1.0E+15 VCD NO_2) were -101% (-105%), -98% (-
478 93%), and -10% (-9%), respectively. The fractional biases for the matched-
479 threshold analysis of the FEPS plume rise scenario were -117% (-125%), -
480 97% (-90%), and -18% (-12%), respectively (Table 4). The biases in total
481 column CO are within the reported retrieval error, and thus are not
482 significant. The low tropospheric NO_2 biases were greater in magnitude than
483 the reported retrieval errors, and mostly driven by the lack of NO_2 coming in
484 from south of the domain. The low AOD biases were much greater in
485 magnitude than the expected retrieval error, indicating persistent problems
486 with AIRPACT-3 aerosol predictions.

487 *3.2 CALIPSO PLUME TOP HEIGHT COMPARISON*

488 CALIOP retrievals were compared to AIRPACT aerosols across the
489 model domain when CALIPSO passed over the Idaho and California wildfire
490 smoke plumes during the analysis periods of 2007 and 2008, respectively.
491 There were many instances where both AIRPACT-3 and CALIOP showed the
492 presence of fire-related aerosol pollution at similar heights. In 2007 (2008),
493 CALIOP retrievals showed aerosol pollution over 328 (383) unique AIRPACT
494 grid cells across Nevada, Idaho, and Canada (California, Oregon,
495 Washington, and Canada), while 218 (281) and 219 (275) of those grid cells
496 had AIRPACT-3 aerosol pollution in the SMOKE and FEPS plume rise
497 scenarios.

498 There was moderate linear correlation (r^2=0.41 for FEPS plume rise;

499 r^2=0.50 for SMOKE plume rise) between AIRPACT-3 and CALIPSO plume top
500 heights AMSL, when both showed the presence of an aerosol subtype (Fig.
501 7). On average, in 2007 (2008) the AIRPACT-3 FEPS plume-rise scenario
502 under-predicted plume top heights AMSL by 3.1±2.3 km (2.5±1.5 km), while
503 the SMOKE plume-rise scenario under-predicted plume top heights AMSL by
504 3.1±2.0 km (2.2±1.6 km). There were many instances in which AGL
505 comparisons were reasonable but dissimilar terrain heights resulted in large
506 under-predictions in plume top heights AMSL. The horizontal resolution of
507 AIRPACT smoothes the surface elevation in complex terrain so that it is
508 consistently lower relative to CALIOP retrievals, and is a large source of
509 uncertainty when evaluating AIRPACT plume tops. We found smaller linear
510 correlation (r^2=0.18 for FEPS plume rise; r^2=0.24 for SMOKE plume rise)
511 between AIRPACT-3 and CALIPSO plume tops heights AGL (Table 5 and Fig.
512 7). On average, though, in 2007 (2008) the AIRPACT-3 FEPS plume-rise
513 scenario under-predicted plume top heights AGL by 1.4±2.3 km (1.0±1.2
514 km) while the SMOKE plume-rise scenario under-predicted plume top heights
515 AGL by 1.5±1.9 km (0.9±1.3 km). This is consistent with a national study
516 using a similar modeling structure, where CMAQ plume heights were under-
517 predicted by ~20%, relative to CALIOP retrievals (Raffuse et al., 2012).

518 *3.3 SURFACE CONCENTRATION RESULTS*

519 From July 3 to Aug. 22, 2007 (June 22 to Aug. 27, 2008) the daily 24-
520 hr average $PM_{2.5}$ was averaged across 67 (82) sites and the maximum daily
521 8-hr average ozone was averaged across 10 (18) sites for modeled and

522 measured concentrations. The "all sites" comparison (Fig. 8) shows that
523 maximum daily 8-hr surface ozone was generally under-predicted by 2 – 8
524 ppb in 2007, which might be expected with simulations of ozone in the
525 presence of aerosols (Alvarado and Prinn, 2009). The maximum daily 8-hr
526 ozone was nearly matched in 2008. In general, AIRPACT-3 predicted
527 changes in ozone that were similar to what was observed across the region.
528 The timeline also shows that AIRPACT-3 generally under-predicted daily
529 surface PM2.5 averages by 2 - 5 $\mu g/m^3$ and followed the measured curve
530 closely except for gross over-prediction of surface $PM_{2.5}$ concentrations from
531 August 14 – 16, 2007 and July 12 – 13, 2008.

532 *3.4 $PM_{2.5}$ NAAQS COMPARISONS*

533 AIRPACT-3 daily 24-hr PM2.5 was assessed from a policy standpoint
534 for both the daily (35 $\mu g/m^3$) and annual (12 $\mu g/m^3$) National Ambient Air
535 Quality Standards (NAAQS) threshold values. For each site, we calculated the
536 number of days when both the model results and the observations showed
537 $PM_{2.5}$ concentrations greater than the NAAQS. We tallied the number of
538 these days during the analysis period, for 67 sites in 2007 and 82 sites in
539 2008. For the FEPS plume-rise scenario we found: 97.7% of the data pairs
540 were in agreement, with values less than the daily threshold; 0.2% of the
541 data pairs were in agreement, with values higher than the daily threshold;
542 0.3% of the data pairs included observations higher than the daily threshold,
543 with no such model prediction; and 1.8% of the data pairs included model
544 predictions higher than the daily threshold, with no such observation. The

545 SMOKE plume-rise scenario reduced the number of model predictions that
546 were higher than the daily threshold, with no such observation, by 27% (or
547 1.3% of the total data pairs).

548 In terms of the annual threshold, the FEPS plume-rise scenario showed
549 that: 90.7% of the data pairs were in agreement, with values less than the
550 annual threshold; 1.8% of the data pairs were in agreement, with values
551 higher than the annual threshold; 4% of the data pairs included observations
552 higher than the annual threshold, with no such model prediction; and 3.5%
553 of the data pairs included model predictions higher than the annual
554 threshold, with no such observations. The SMOKE plume-rise scenario
555 increased the number of data pairs that were in agreement, with values
556 higher than the annual threshold, by 17% (2.1% of the total data pairs).
557 Further details of the $PM_{2.5}$ NAAQS comparison are in Table 6 and Figs. S9-
558 S10.

559 *3.5 MT. BACHELOR OBSERVATORY COMPARISON*

560 Hourly observed and predicted AIRPACT-3 values for PM, carbon
561 monoxide, and ozone at Mt. Bachelor Observatory during the 2008 California
562 wildfires (Fig. 9) show how AIRPACT-3 generally does with medium-range
563 transport of wildfire emissions. There is evidence of model under-prediction,
564 especially in the FEPS plume-rise scenario, but the SMOKE plume-rise
565 scenario resulted in over-prediction of CO for most fire events. There was
566 generally good agreement of the timing of pollution events but occasionally
567 the timing was off by a day, as occurred on August 8-9 (Fig. 9). Note that PM

568 for AIRPACT-3 in the Mt. Bachelor analysis is reported as $PM_{2.5}$ but the
569 observations are of sub-micron aerosols converted from scattering
570 observations using the method described in Wigder et al., (2013), which can
571 have large uncertainty when there is significant variance in the aerosol size
572 distribution (Akagi et al., 2012).

573 On July 20, 2008, there was a large transport event that carried
574 pollutants northwest from the fires in California until reaching the coast of
575 Oregon where the plume was diverted inland to the northeast, sweeping
576 across Oregon (Figs. 6, S8, S11). MBO measurements of sub-micron PM
577 were between 80 and 120 $\mu g/m^3$ from midnight to noon, and between 20 and
578 45 $\mu g/m^3$ for the proceeding 24 hours. AIRPACT-3 predictions of carbon
579 monoxide and $PM_{2.5}$ were well timed with monitor observations, but the
580 AIRPACT-3 FEPS plume-rise scenario consistently under-predicted CO and PM
581 concentrations during the event while the SMOKE plume rise scenario did
582 better on average but still under-predicted PM. The event did not have
583 emissions from outside the domain that significantly contributed to the
584 plume, but some model aerosols were clearly lost to the domain boundary.
585 However, the aerosol transported out of the boundary was not enough to
586 explain well-predicted carbon monoxide combined with 30%-50% under-
587 predictions in PM. There was a smaller event with similar comparisons
588 between observations and predictions on July 25, 2008 as well. Throughout
589 the 2008 MBO analysis dates, AIRPACT-3 generally under-predicted aerosols
590 when CO was predicted well and over-predicted CO when aerosols were

predicted well. This is consistent with other observations that show AIRPACT-3 PM2.5/CO ratios to be low at locations greater than ~100 km from the fire location. Observations on July 20, July 25, and August 9 resulted in PM1/CO ratios of ~0.3 ug/m^3/ppbv, higher than the ratios observed for fires in closer proximity to MBO, which has been previously interpreted to indicate SOA formation during plume transport (Wigder et al., 2013).

The remote sensing comparison of the unique event on July 20, 2008 confirmed a consistent negative bias in predicted transported aerosols, even where CO in the SMOKE plume-rise scenario agreed well with AIRS. MODIS observed AOD values as high as 1.2 directly northwest of MBO, with lower values near 0.4 directly over the site. AIRPACT-3 only predicted AOD of 0.1 to 0.4 through the region of the large plume over those same regions around MBO (Fig. 6). AIRS also retrieved good quality carbon monoxide columns west of MBO, in the more concentrated part of the plume, showing a model under-bias of ~10%. Tropospheric NO_2 columns over the transported portion of the plume were below the signal to noise threshold of OMI.

4 Discussion

AIRPACT-3 correctly predicted which regions were impacted by fires in Idaho, Montana, Nevada, California, and Oregon during the summers of 2007 and 2008. This is reflected in the comparisons to AIRS carbon monoxide, OMI tropospheric NO_2, and MODIS AOD, which all exhibited good

613 spatiotemporal correlation to AIRPACT-3. General model performance was
614 quite similar between the two years, which suggests that the differences
615 from using MM5 in 2007 and WRF in 2008 did not have a significant effect on
616 the chemical transport modeling during the fire events.

617 The SMOKE plume-rise scenario exhibited the best comparisons, with
618 average fractional biases at ~2 p.m. for AOD, tropospheric column NO_2 and
619 total column CO found to be -61%, -39%, and -10% during the 2007 fire
620 period, respectively; while during the 2008 fire period the average fractional
621 biases were -53%, -28%, and -5% respectively. Surface concentrations of
622 $PM_{2.5}$ were also reasonable, especially in the SMOKE plume rise scenarios,
623 which lifted some of the surface emissions aloft and constrained large plume
624 top heights. The fractional bias of daily average 24-hr PM2.5 was found to
625 be approximately -30% during both fire periods. Fractional biases of
626 AIRPACT-3 plume tops were found to be -46% above mean sea level (AMSL),
627 but only -28% above ground level (AGL), partly due to the under-estimation
628 of AIRPACT-3 elevation in complex terrain. Underestimation of plume
629 heights, which affects transport, may be partly responsible for under-
630 prediction in transported aerosols. However, the under-prediction of SOA in
631 model simulations is likely the largest source of model error, especially when
632 we consider that other species, such as CO, were not under-predicted by
633 such large magnitudes.

634 Fire emissions generated from south of the domain were not well
635 represented in AIRPACT-3 chemical boundary conditions derived from

636 MOZART-4; a few events in 2008 appeared to be significantly affected by
637 those under-predictions in boundary condition concentrations. This is
638 consistent with the analysis of Pfister et al. (2011) that showed FINN
639 emission factors were too low in the 2008 California fire simulations due to a
640 misclassification of fuel type. MOZART-4 showed general agreement with the
641 background values of CO and O_3 (Fig. 9), but missed the high values
642 expected from fires due to the coarse model resolution and the
643 underestimation of fire emissions and plume height. Thus AIRPACT-3 model
644 performance would benefit from revised methods to better represent fire
645 influence on AIRPACT-3 boundary conditions.

646 Comparisons of AIRPACT-3 plumes with CALIOP show that the
647 dynamics of plume dispersion in the model are greatly affected by errors in
648 surface terrain and vertical plume distribution and their interaction with the
649 wind profiles. There is also evidence that the underestimation of terrain
650 height in AIRPACT-3 and the overestimation of plume-top heights AGL could
651 be compensating errors in some of the FEPS plume rise scenarios.

652 AIRPACT-3 tropospheric NO_2 was generally under-predicted, but there
653 were occasionally what appeared to be large overestimates of tropospheric
654 NO_2 over active fire regions (Figs. S5a, S5b, S7a, S7b). It is important to
655 note that these large tropospheric NO_2 predictions shown are a direct result
656 of our application of the OMI averaging kernel, which weights the upper
657 troposphere with a factor greater than one. In most cases, the plumes are
658 low enough to the ground that the averaging kernel causes a net reduction in

AIRPACT-3 tropospheric NO_2 columns. However, in cases where FEPS considerably over-predicted plume top height, the modeled tropospheric NO_2 column convolved with the averaging kernel caused a spike much higher than that of the original AIRPACT-3 results. The effect still occurs in the SMOKE plume rise scenario, though there are fewer extreme instances. Furthermore, the OMI tropospheric NO_2 algorithms have large errors over wildfires due to a combination of the a priori profiles used that assume NO_2 is concentrated near the surface, the high aerosol loadings emitted, and issues with comparisons over complex terrain (Boersma et al., 2011).

Collectively, the results of this analysis show that AIRPACT-3 can over-predict surface fire emissions and occasionally under-predict fire emissions aloft which, coupled with discrepancies in modeled surface elevation, significantly affects the ability of AIRPACT-3 to accurately predict downwind surface concentrations of transported pollutants in complex terrain. Our analysis shows that AIRPACT-3 CO performs quite well when compared to surface concentrations (Fig 9) and AIRS total column retrievals (Figs. 5, 6, S5a, S5b). This is in contrast to the frequent underestimates of transported aerosols that were evident in AIRPACT-3 predictions of surface PM2.5 (Fig. 9) and AOD (Figs. 4, 5, 6, S5a). Satellite comparisons clearly show that when modeled CO across the domain is largely in close agreement with observations, aerosol performance systematically degrades with distance from the fire source. Akagi et al. (2011) and Yokelson et al. (2013) suggest that the emission factors for VOCs used in CONSUME-3 (Hardy, 1996 and

682 Ward et al., 1989) should be much higher. This underestimation in VOC
683 emissions further exacerbates known under-predictions of SOA in CMAQ,
684 which can be a significant fraction of the total PM2.5 for plumes transported
685 large distances (Wigder et al., 2013; Strand et al., 2012; Hu et al., 2008;
686 Heilman et al., 2013) and is highly variable (Jolleys et al., 2012; Yokelson et
687 al., 2009; Vakkari et al., 2014).

688 **5 Conclusions & Future Work**

689 In general, AIRPACT-3 over-predicts pollutant concentrations due to
690 near-source surface emissions from fires and under-predicts concentrations
691 associated with long-range transport both from within the domain and
692 outside the domain. Most fire locations are captured by the BlueSky
693 SMARTFIRE tool, but there are occasionally fires predicted that are poorly
694 timed or are missed. Our analysis suggests that total fire emissions in the
695 domain are, overall, modestly under-predicted. Although we have shown
696 that AIRPACT-3 chemical boundary conditions largely underestimate fire-
697 emissions from outside the domain, this problem does not explain most
698 under-predictions that occur at ground sites. The under-predictions are
699 instead likely due to a combination of some or all of the following: 1)
700 underestimates of area burned in the SMARTFIRE feed; 2) underestimates of
701 fuel mass, especially in shrub-lands and other vegetation types that have
702 sparse woody fuels but are classified with zero dead woody fuels in the
703 FCCS; 3) underestimates of VOC emissions in the Consume model; 4) under-
704 predictions of SOA production in CMAQ, thus causing under-predictions of PM

705 in plumes that travel large distances; and 5) terrain height in the AIRPACT-3
706 model is too smooth in mountainous areas, causing problems with the
707 elevation of emissions and dynamics of transport. Under-predictions in fire
708 size also scale directly with under-predictions in plume top heights, since
709 heat content of a fire is directly proportional to the total fuel in Consume,
710 which adds uncertainty to predictions of transport.

711 The high-resolution MODIS AOD retrievals provided considerable
712 insight into AIRPACT aerosol performance. We also feel that alternative
713 retrieval algorithms better suited for fire plume conditions might address
714 some of the errors associated with AIRS and OMI trace gas comparisons.
715 Furthermore, we recognize that coupling fire dynamics with meteorological
716 simulations, such as in the WRF-Fire framework (Coen et al., 2013;
717 Kochanski et al., 2013; Mandel et al., 2011) may be the best method for
718 forecasts once WRF-Fire simulations can be generated fast enough. We
719 have recently updated the system to AIRPACT-4, which includes 4 km x 4 km
720 horizontal grid cells and the SMOKE plume-rise method, in addition to
721 updated BlueSky software which includes higher resolution fuel loading in
722 FCCS and an updated SMARTFIRE (v2). Canadian fires within the model
723 domain will be included, starting in 2015, but AIRPACT-4 would still benefit
724 by having chemical boundary conditions that accurately represent smoke
725 originating from outside the AIRPACT domain. Planned updates to the
726 AIRPACT vertical layer spacing in the middle troposphere should also help
727 model performance during fire emissions transport events.

6 Acknowledgments

This research was made possible by a NASA grant (NNX11AE57G) and was also partially supported by a grant from the National Science Foundation's REU program (0754990). The National Center for Atmospheric Research is funded by the National Science Foundation and operated by the University Corporation for Atmospheric Research. The Mt. Bachelor Observatory is supported by the National Science Foundation (AGS-1066032AM002). NW-AIRQUEST provides support for the operation of the AIRPACT forecast system. We would also like to thank Matthew Mavko and other affiliates of the Western Regional Air Partnership.

7 References

Akagi, S. K., Yokelson, R. J., Wiedinmyer, C., Alvarado, M. J., Reid, J. S., Karl, T., Crounse, J. D., and Wennberg, P. O.: Emission factors for open and domestic biomass burning for use in atmospheric models, Atmos. Chem. Phys., 11, 4039-4072, doi:10.5194/acp-11-4039-2011, 2011.

Akagi, S. K., Craven, J. S., Taylor, J. W., McMeeking, G. R., Yokelson, R. J., Alvarado, M. J., Logan, J. A., Mao, J., Apel, E., Riemer, D., Blake, D., Cohen, R. C., Min, K.-E., Perring, A. E., Browne, E. C., Wooldridge, P. J., Diskin, G. S., Sachse, G. W., Fuelberg, H., Sessions, W. R., Harrigan, D. L., Huey, G., Liao, J., Case-Hanks, A., Jimenez, J. L., Cubison, M. J., Vay, S. A., Weinheimer, A. J., Knapp, D. J., Montzka, D. D., Flocke, F. M., Pollack, I. B., Wennberg, P. O., Kurten, A., Crounse, J., Clair, J. M. St., Wisthaler, A., Mikoviny, T., Yantosca, R. M., Carouge, C. C., and Le Sager, P.: Nitrogen oxides and PAN in plumes from boreal fires during ARCTAS-B and their impact on ozone: an integrated analysis of aircraft and satellite observations, Atmos. Chem. Phys., 10, 9739-9760, doi:10.5194/acp-10-9739-2010, 2010.

.

Ambrose, J.L., Reidmiller, D.R., and Jaffe, D.A.: Causes of high O3 in the lower free troposphere over the Pacific Northwest as observed at the Mt. Bachelor Observatory, Atmospheric Environment. DOI: 10.1016/j.atmosenv.2011.06.056, 2011.

763 Anderson, G.K., Sandberg, D.V., and Norheim, R.A. : Fire Emission
764 Production Simulator (FEPS) User's Guide, Joint Fire Science Program and the
765 National Fire Plan, January, 2004.
766
767 Bhoi, S., Qu, J.J., Dasgupta, S. (2009). Multi-sensor study of aerosols from
768 2007 Okefenokee forest fire. *Journal of Applied Remote Sensing,* Vol. 3,
769 031501, DOI:10.1117/1.3078070.
770
771 Binkowski, F. S., & Roselle, S. J. (2003). Models-3 Community Multiscale Air
772 Quality (CMAQ) model aerosol component 1. Model description. *Journal of*
773 *Geophysical Research, 108. doi:10.1029/2001JD001409.*
774
775 Boersma, K.F., H.J. Eskes, J.P. Veefkind, E.J. Brinksma, R.J. van der A, M.
776 Sneep, G.H.J. van den Oord, P.F. Levelt, P. Stammes, J.F. Gleason and E.J.
777 Bucsela, Near-real time retrieval of tropospheric NO2 from OMI, Atm. Chem.
778 Phys., 2013-2128, sref:1680-7324/acp/2007-7-2103, 2007
779
780 Boersma, K. F., H. J. Eskes, R. J. Dirksen, R. J. van der A, J. P. Veefkind, P.
781 Stammes, V. Huijnen, Q. L. Kleipool, M. Sneep, J. Claas, J. Leitao, A. Richter,
782 Y. Zhou, and D. Brunner (2011). An improved retrieval of tropospheric NO2
783 columns from the Ozone Monitoring Instrument, Atmos. Meas. Tech., 4,
784 1905-1928, 2011
785
786 Burling, I. R., Urbanski, S. P., Wold, C. E., Seinfeld, J. H., Coe, H., Alvarado,
787 M. J., and Weise, D. R.: Evolution of trace gases and particles emitted by a
788 chaparral fire in California, Atmos. Chem. Phys., 12, 1397-1421,
789 doi:10.5194/acp-12-1397-2012, 2012
790
791 Byun, D. and Schere, K. L.: Review of the Governing Equations,
792 Computational Algorithms, and other components of the models-3
793 community multiscale air quality (CMAQ) modeling system, Applied
794 Mechanics Review, Vol. 59, March 2006.
795
796 Calipso User Guide: CALIPSO Lidar Level-2 5 km Vertical Feature Mask (VFM)
797 Products, NASA Langley Research Center, Accessed on October 6, 2011 at
798 http://www-
799 calipso.larc.nasa.gov/resources/calipso_users_guide/data_summaries/vfm/
800
801 Chen, J., J. Vaughan, J. Avise, S. O'Neill, and B. Lamb (2008), Enhancement
802 and evaluation of the AIRPACT ozone and PM2.5 forecast system for the
803 Pacific Northwest, J. Geophys. Res., 113, D14305,
804 doi:10.1029/2007JD009554.
805
806 Christopher, S., P. Gupta, U. Nair, T. A. Jones, S. Kondragunta, Y-L Wu, J.
807 Hand, and X. Zhang (2009), Satellite Remote Sensing and Mesoscale
808 Modeling of the 2007 Georgia/Florida Fires, *IEEE J. of Selected Topics in*
809 *Applied Earth Sciences and Remote Sensing*.
810

811 Coen, J., M. Cameron, J. Michalakes, E. Patton, P. Riggan, and K. Yedinak,
812 2013: WRF-Fire: Coupled Weather-Wildland Fire Modeling with the Weather
813 Research and Forecasting Model. J. Appl. Meteor. Climatol. 52, 16-38,
814 doi:10. 1175/JAMC-D-12-023.1
815
816 Deeter, M. N., et al., The MOPITT version 4 CO product: Algorithm
817 enhancements, validation, and long- term stability , J. Geophys. Res., 115 ,
818 D07306, doi:10.1029/2009JD013005, 2010.
819
820 Drury, E., D. J. Jacob, J. Wang, R. J. D. Spurr, and K. Chance (2008),
821 Improved algorithm for MODIS satellite retrievals of aerosol optical depths
822 over western North America, J. Geophys. Res., 113, D16204,
823 doi:10.1029/2007JD009573.
824
825 Eck, T. F., Holben, B. N., Reid, J. S., Mukelabai, M. M., Piketh, S. J., Torres,
826 O., Jethva, H. T., Hyer, E. J., Ward, D. E., Dubovik, O., Sinyuk, A., Schafer,
827 J.S., Giles, D. M., Sorokin, M., Smirnov, A. and Slutsker, I.: A seasonal trend
828 of single scattering albedo in southern African biomass-burning particles:
829 Implications for satellite products and estimates of emissions for the world's
830 largest biomass-burning source, Journal of Geophysical Research:
831 Atmospheres, Volume 118, Issue 12, 27 June 2013, Pages: 6414–6432, DOI:
832 10.1002/jgrd.50500
833
834 Emmons, L. K., Walters, S., Hess, P. G., Lamarque, J.-F., Pfister, G. G.,
835 Fillmore, D., Granier, C., Guenther, A., Kinnison, D., Laepple, T., Orlando, J.,
836 Tie, X., Tyndall, G., Wiedinmyer, C., Baughcum, S. L., and Kloster, S.:
837 Description and evaluation of the Model for Ozone and Related chemical
838 Tracers, version 4 (MOZART-4), Geosci. Model Dev., 3, 43-67,
839 doi:10.5194/gmd-3-43-2010, 2010.
840
841 Engel-Cox, J.A., Holloman, C.H., Coutant, B.W., Hoff, R.M.: Qualitative and
842 quantitative evaluation of MODIS satellite sensor data for regional and urban
843 scale air quality, Atmospheric Environment, Volume 38, Issue 16, May 2004,
844 Pages 2495-2509, ISSN 1352-2310, 10.1016/j.atmosenv.2004.01.039.
845
846 Evans, T. N., & Fournier, G. R. (1990). Simple approximation to extinction
847 efficiency valid over all size range. *Applied Optics, 29, 4666-4670.*
848
849 Green, M., Kondragunta, S., Ciren, P., Xu, C.: Comparison of GOES and
850 MODIS Aerosol Optical Depth (AOD) to AErosol RObotic NETwork (AERONET)
851 AOD and IMPROVE PM2.5 mass at Bondville, Illinois, *Journal of the Air &*
852 *Waste Management Association* , vol. 59, no. 9, pp. 1082-1091, 2009
853 doi:10.3155/1047-3289.59.9.1082
854
855 Hardy, C. 1996. Guidelines for Estimating Volume, Biomass, and Smoke
856 Production for Piled Slash. Gen. Tech. Rep PNW-GTR-364. Portland, OR: U.S.
857 Department of Agriculture, Forest Service, Pacific Northwest Research
858 Station.

Heilman, W.E., et al. Wildland fire emissions, carbon, and climate: Plume rise, atmospheric transport, and chemistry processes. Forest Ecol. Manage. (2013), http://dx.doi.org/10.1016/j.foreco.2013.02.001

Herron-Thorpe, F. L., Lamb, B. K., Mount, G. H., and Vaughan, J. K.: Evaluation of a regional air quality forecast model for tropospheric NO_2 columns using the OMI/Aura satellite tropospheric NO_2 product, Atmos. Chem. Phys., 10, 8839-8854, doi:10.5194/acp-10-8839-2010, 2010.

Herron-Thorpe, F. L., Mount, G. H., Emmons, L. K., Lamb, B. K., Chung, S. H., and Vaughan, J. K.: Regional air-quality forecasting for the Pacific Northwest using MOPITT/TERRA assimilated carbon monoxide MOZART-4 forecasts as a near real-time boundary condition, Atmos. Chem. Phys., 12, 5603-5615, doi:10.5194/acp-12-5603-2012, 2012.

Hoff, R. M. "Remote sensing of particulate pollution from space: have we reached the promised land." Journal of the Air & Waste Management Association 59(2009):645.

Hu, Yongtao, M. Talat Odman, Michael E. Chang, William Jackson, Sangil Lee, Eric S. Edgerton, Karsten Baumann, and Armistead G. Russell: Simulation of Air Quality Impacts from Prescribed Fires on an Urban Area Environmental Science & Technology 2008 42 (10), 3676-3682

Jolleys, M.D., Coe, H., McFiggans, G., Capes, G., Allan, J.D., Crosier, J., Williams, P.I., Allen, G., Bower, K.N., Jimenez, J.L., Russell, L.M., Grutter, M., Baumgardner, D., 2012. Characterizing the aging of biomass burning organic aerosol by use of mixing ratios: a meta-analysis of four regions. Environmental Science & Technology 46, 13093e13102

Kahn, R. A. "Wildfire smoke injection heights: Two perspectives from space." Geophysical research letters 35(2008):L04809.

Kahn, R. A., B. J. Gaitley, M. J. Garay, D. J. Diner, T. Eck, A. Smirnov, and B. N. Holben (2010), Multiangle imaging Spectroradiometer global aerosol product assessment by comparison with the aerosol robotic network. J. Geophys. Res. 115, D23209, doi:10.1029/2010JD014601.

Kochanski, A.K., Jenkins, M.A., Krueger, S.K., Mandel, J., and Beezley, J.D., 2013: Real time simulation of 2007 Santa Ana fires, Forest Ecology and Management 15, 136-149, 2013 doi:10.1016/j.foreco.2012.12.014 arXiv:1202.3209

Larkin, N.K., S.M. O'Neill, R. Solomon, S. Raffuse, T. Strand, D.C. Sullivan, C. Krull, M. Rorig, J. Peterson and S.A. Ferguson: The BlueSky smoke modeling framework, International Journal of Wildland Fire 18(8)

906–920 (2009)

Levy, R. C., Remer, L. A., Mattoo, S., Vermote, E. F., and Kaufman, Y. J.: Second-generation operational algorithm: Retrieval of aerosol properties over land from inversion of Moderate Resolution Imaging Spectroradiometer spectral reflectance, J. Geophys. Res., 112, D13211, http://dx.doi.org/10.1029/2006JD007811doi:10.1029/2006JD007811, 2007b.

Maddy, E. S. and Barnet, C. D.: Vertical resolution estimates in version 5 of AIRS operational retrievals, IEEE Transactions on Geoscience and Remote Sensing, 46, 8, doi:10.1109/TGRS.2008.917498, 2008.

Mandel, J., Beezley, J.D., and Kochanski, A.K.: Coupled atmosphere-wildland fire modeling with WRF 3.3 and SFIRE 2011, Geoscientific Model Development (GMD) 4, 591-610, 2011. doi:10.5194/gmd-4-591-2011

Mass, C. F., M. Albright, D. Ovens, R. Steed, M. MacIver, E. Grimit, T. Eckel, B. Lamb, J. Vaughan, K. Westrick, P. Storck, B. Colman, C. Hill, N. Maykut, M. Gilroy, S. A. Ferguson, J. Yetter, J. M. Sierchio, C. Bowman, R. Stender, R. Wilson and W. Brown, 2003: Regional Environmental Prediction over the Pacific Northwest, The Bulletin of the American Meteorological Society, 84, 1353-1366.

Mielonen, T., A. Arola, M. Komppula, J. Kukkonen, J. Koskinen, G. de Leeuw, and K. E. J. Lehtinen (2009), Comparison of CALIOP level 2 aerosol subtypes to aerosol types derived from AERONET inversion data, *Geophys. Res. Lett.*, *36*, L18804, doi:10.1029/2009GL039609.

Olsen, E.T., Fishbein, E., Lee, S.Y., Manning, E., Maddy, E., and McMillan, W. W.: AIRS/AMSU/HSB Version 5 Level 2 Product Levels, Layers and Trapezoids, Retrieval Channel Sets, Jet Propulsion Laboratory, California Institute of Technology, Pasadena, CA, 2007.

Omar, Ali H., and Coauthors, 2009: The CALIPSO Automated Aerosol Classification and Lidar Ratio Selection Algorithm. *J. Atmos. Oceanic* Technol., 26, 1994–2014. doi: 10.1175/2009JTECHA1231.1

Ottmar, Roger; Miranda, Ana; Sandberg, David. 2009. Characterizing sources of emissions from wildland fires. In: Bytnerowicz, Andrzej; Arbaugh, Michael; Riebau, Allen; Andersen, Christian, eds. Wildland fires and air pollution. Amsterdam: Elsevier: 61-78. Chapter 3. (Developments in Environmental Science Series Volume 8).

Pfister, G. G., Avise, J., Wiedinmyer, C., Edwards, D. P., Emmons, L. K., Diskin, G. D., Podolske, J., and Wisthaler, A.: CO source contribution analysis for California during ARCTAS-CARB, Atmos. Chem. Phys., 11, 7515-7532, doi:10.5194/acp-11-7515-2011, 2011.

Pouliot, G., Pierce, T., Benjey, W., O'Neill, S.M., Ferguson, S.A., 2005. Wildfire emission modeling: integrating BlueSky and SMOKE. Presentation at the 14th International Emission Inventory Conference, Transforming Emission Inventories Meeting Future Challenges Today, 4 /11 –4/14/05 Las Vegas, NV.

Raffuse, S. M., D. A. Pryden, D. C. Sullivan, N. K. Larkin, T. Strand, and R. Solomon. (2009), SMARTFIRE algorithm description, report, Sonoma Technol., Inc., Petaluma, Calif.

Raffuse, S. M., Craig, K. J., Larkin, N. K., Strand, T. T., Sullivan, D. C., Wheeler, N. J. M. and Solomon, R.: An evaluation of modeled plume injection height with satellite-derived observed plume height, Atmosphere, 3(4), 103–123, doi:10.3390/atmos3010103, 2012.

Remer, L. A., and Coauthors, 2005: The modis aerosol algorithm, products, and validation. *J. Atmos. Sci.*, 62, 947–973. doi: 10.1175/JAS3385.1

Riccardi, Cynthia L.; Prichard Susan J.; Sandberg, David V.; Ottmar, Roger D. (2007). Quantifying Physical Characteristics of Wildland Fuels Using the Fuel Characteristic Classification System, Canadian Journal of Forest Research. 37(12): 2413-2420.

Roy, B., R. Mathur, A. B. Gilliland, and S. C. Howard (2007), A comparison of CMAQ-based aerosol properties with IMPROVE, MODIS, and AERONET data, *J. Geophys. Res.*, 112, D14301, doi:10.1029/2006JD008085.

Seinfeld J. H. and Pandis S. N. (1998) Atmospheric Chemistry and Physics: From Air Pollution to Climate Change, J. Wiley, New York.

Simon, H. and Bhave, P.V., 2012. Simulating the degree of oxidation in atmospheric organic particles, Environ. Sci. Technol., 46(1), 331-339.

Skamarock, W. C., J. B. Klemp, J. Dudhia, D. O.Gill, D. M. Barker, W. Wang, J. G. Powers (2005), A Description of the Advanced Research WRF Version 2. Boulder, Colorado: National Center for Atmospheric Research.

Strand, T., Larkin N.K., Rorig M., Krull C., Moore M. 2011. PM2.5 measurements in wildfire smoke plumes from fire seasons 2005-2008 in the Northwestern United States. Journal of Aerosol Science, 42, 3, 143-155.

Strand, T. M., Larkin, N., Solomon, R., Rorig, N., Craig, K. J., Raffuse, S., Sullivan, D., Wheeler, N., and Pryden, D. (2012) Analyses of BlueSky Gateway PM2.5 predictions during the 2007 southern and 2008 northern California fires. J. Geophys. Res., 117, D17301, doi:10.1029/2012JD017627.

Vakkari, V., Kerminen, V.-M., Beukes, J.P., Tiitta, P., van Zyl, P.G., Josipovic, M., Venter, A., Jaars, K., Worsnop, D., Kulmala, M., and Laakso, L., Rapid changes in biomass burning aerosols by atmospheric oxidation, Geophys. Res. Lett., 41, doi:10.1002/2014GL059396, 2014

Vaughan, M., Winker, D., and Powell, K.: CALIOP Algorithm Theoretical Basis Document, part 2, Feature detection and layer properties algorithms, PC-SCI-202.01, NASA Langley Res. Cent., Hampton, Va., 2005 (available at http://www-calipso.larc.nasa.gov/resources/project_documentation.php) 3771

Weiss-Penzias, P., D. A. Jaffe, P. Swartzendruber, J. B. Dennison, D. Chand, W. Hafner, and E. Prestbo; Observations of Asian air pollution in the free troposphere at Mt. Bachelor Observatory in the spring of 2004, J. Geophys. Res., 110, D10304, doi:10.1029/2005JD006522, 2006.

Wespes, C., Emmons, L., Edwards, D. P., Hannigan, J., Hurtmans, D., Saunois, M., Coheur, P.-F., Clerbaux, C., Coffey, M. T., Batchelor, R. L., Lindenmaier, R., Strong, K., Weinheimer, A. J., Nowak, J. B., Ryerson, T. B., Crounse, J. D., and Wennberg, P. O.: Analysis of ozone and nitric acid in spring and summer Arctic pollution using aircraft, ground-based, satellite observations and MOZART-4 model: source attribution and partitioning, Atmos. Chem. Phys., 12, 237-259, doi:10.5194/acp-12-237-2012, 2012.

Wiedinmyer, C., Akagi, S. K., Yokelson, R. J., Emmons, L. K., Al- Saadi, J. A., Orlando, J. J., and Soja, A. J.: The Fire INventory from NCAR (FINN): a high resolution global model to estimate the emissions from open burning, Geosci. Model Dev., 4, 625– 641, doi:10.5194/gmd-4-625-2011, 2011.

Ward, D.E., Hardy, C.C., Sandberg, D.V., Reinhardt, T.E. 1989. Part III-emissions characterization, In Sandberg, D.V.; Ward, D.E.; Ottmar, R.D., comps. Mitigation of prescribed fire atmospheric pollution through increased utilization of hardwoods, piled residues, and long-needled conifers. Final report;. U.S. DOE, BPA. Available from U.S. Department of Agriculture, Forest Service, Pacific Northwest Research Station, Seattle, WA.

Wigder, N.L., Jaffe, D.A., Saketa, F.A., Ozone and Particulate Matter Enhancements from Regional Wildfires Observed at Mount Bachelor during 2004-2011, *Atmos. Environ* (2013), doi: 10.1016/j.atmosenv.2013.04.026

Winker, David M., Mark A. Vaughan, Ali Omar, Yongxiang Hu, Kathleen A. Powell, Zhaoyan Liu, William H. Hunt, Stuart A. Young, 2009: Overview of the CALIPSO Mission and CALIOP Data Processing Algorithms. *J. Atmos. Oceanic Technol.*, 26, 2310–2323. doi: 10.1175/2009JTECHA1281.1

Wong, D. C., Pleim, J., Mathur, R., Binkowski, F., Otte, T., Gilliam, R., Pouliot, G., Xiu, A., Young, J. O., and Kang, D.: WRF-CMAQ two-way coupled

system with aerosol feedback: software development and preliminary results, Geosci. Model Dev., 5, 299-312, doi:10.5194/gmd-5-299-2012, 2012.

Yokelson, R. J., Crounse, J. D., DeCarlo, P. F., Karl, T., Urbanski, S., Atlas, E., Campos, T., Shinozuka, Y., Kapustin, V., Clarke, A. D., Weinheimer, A., Knapp, D. J., Montzka, D. D., Holloway, J., Weibring, P., Flocke, F., Zheng, W., Toohey, D., Wennberg, P. O., Wiedinmyer, C., Mauldin, L., Fried, A., Richter, D., Walega, J., Jimenez, J. L., Adachi, K., Buseck, P. R., Hall, S. R., and Shetter, R.: Emissions from biomass burning in the Yucatan, Atmos. Chem. Phys., 9, 5785-5812, doi:10.5194/acp-9-5785-2009, 2009.

Yokelson, R. J., Burling, I. R., Gilman, J. B., Warneke, C., Stockwell, C. E., de Gouw, J., Akagi, S. K., Urbanski, S. P., Veres, P., Roberts, J. M., Kuster, W. C., Reardon, J., Griffith, D. W. T., Johnson, T. J., Hosseini, S., Miller, J. W., Cocker III, D. R., Jung, H., and Weise, D. R.: Coupling field and laboratory measurements to estimate the emission factors of identified and unidentified trace gases for prescribed fires, Atmos. Chem. Phys., 13, 89-116, doi:10.5194/acp-13-89-2013, 2013.

8 Tables & Figures

Table 1: Total annual fires and acres burned by state

	2007		2008	
State	**Total Fires**	**Total Acres**	**Total Fires**	**Total Acres**
California	10,034	1,160,297	6,670	1,456,758
Idaho	2,064	2,226,769	1,546	225,832
Montana	2,342	859,977	1,749	211,593
Nevada	924	905,237	491	90,868
Oregon	3,424	758,740	2,561	252,671
Utah	1,527	664,754	1,139	66,170
Washington	2,578	249,708	1,418	154,368
USA Grand Totals	110,237	12,899,948	88,059	7,433,094

NIFC Sources:
http://www.nifc.gov/fireInfo/fireInfo_stats_YTD2007.html
http://www.nifc.gov/fireInfo/fireInfo_stats_YTD2008.html

Table 2: Definitions of Model Comparison Statistics (Chen et al., 2008)

Measured Concentration	O_i
Predicted Concentration	M_i
Number of Paired Data Points	N

Predicted Mean ($\overline{M}$)	$\frac{1}{N}\sum_{i=1}^{N} M_i$
Measured Mean ($\overline{O}$)	$\frac{1}{N}\sum_{i=1}^{N} O_i$
Mean Bias (MB)	$\frac{1}{N}\sum_{i=1}^{N} (M_i - O_i)$
Mean Error (ME)	$\frac{1}{N}\sum_{i=1}^{N} \lvert M_i - O_i \rvert$
Normalized Mean Bias (NMB)	$\frac{1}{N}\sum_{i=1}^{N} \frac{(M_i - O_i)}{O_i}$
Normalized Mean Error (NME)	$\frac{1}{N}\sum_{i=1}^{N} \frac{\lvert M_i - O_i \rvert}{O_i}$
Fractional Bias (FB)	$\frac{1}{N}\sum_{i=1}^{N} \frac{(M_i - O_i)}{0.5(M_i + O_i)}$
Fractional Error (FE)	$\frac{1}{N}\sum_{i=1}^{N} \frac{\lvert M_i - O_i \rvert}{0.5(M_i + O_i)}$
Correlation Coefficient (r)	$\frac{\sum_{i=1}^{N}(M_i - \overline{M})(O_i - \overline{O})}{\left[\sum_{i=1}^{N}(M_i - \overline{M})^2 \cdot \sum_{i=1}^{N}(O_i - \overline{O})^2\right]^{\frac{1}{2}}}$

Table 3: Summary of FEPS plume-rise scenario comparisons (SMOKE plume-rise scenario shown in parentheses when different) from July 3 to August 23, 2007 (top) and June 22 to August 27, 2008 (bottom).

July 3 - Aug. 22, 2007

Species	A24-hr PM2.5 ($\mu g/m^3$)	MDA8-hr Ozone (ppbV)	AOD	Tot. Col. CO (E+18 molec./cm^2)	Trop. Col. NO_2 (E+15 molec./cm^2)
Observations Source	**EPA AQS**	**EPA AQS**	**MODIS**	**AIRS**	**OMI**
Paired Points	3267	450	3603	4275	5821
Correlation (r)	0.5 (0.6)	0.7	0.4 (0.3)	0.6 (0.5)	0.4
Measured Mean	7.1	45.8	0.2	1.8	1.4
Mean Bias	0.4 (-0.72)	-4.6 (-3.5)	-0.1	-0.2	-0.5
Mean Error	5.6 (4.1)	8.9 (9.0)	0.1	0.2	0.9
Normalized Mean Bias (%)	-2 (-9)	-7 (-4)	-23 (-15)	-12 (-9)	110 (104)
Normalized Mean Error (%)	63 (54)	20 (21)	77 (85)	13 (12)	189 (182)
Fractional Bias (%)	-34 (-33)	-10 (-8)	-66 (-61)	-13 (-10)	-38 (-39)
Fractional Error (%)	60 (57)	22 (21)	91 (90)	14 (13)	75 (76)

June 22 -Aug. 27, 2008

Species	A24-hr PM2.5 ($\mu g/m^3$)	MDA8-hr Ozone (ppbV)	AOD	Tot. Col. CO (E+18 molec./cm^2)	Trop. Col. NO_2 (E+15 molec./cm^2)
Observations Source	**EPA AQS**	**EPA AQS**	**MODIS**	**AIRS**	**OMI**
Paired Points	5329	1135	5125	4577	7760
Correlation (r)	0.0 (0.4)	0.8	0.3	0.7 (0.6)	0.5
Measured Mean	6.8	42.3	0.2	1.9	1.3
Mean Bias	0.3 (-0.7)	-0.7 (0.2)	-0.1	-0.1	-0.3
Mean Error	5.4 (4.1)	7.7 (8.0)	0.1	0.2	0.8
Normalized Mean Bias (%)	34 (5)	3 (5)	-9 (18)	-7 (-4)	110 (106)
Normalized Mean Error (%)	98 (66)	21	85 (108)	9	176 (173)
Fractional Bias (%)	-31 (-27)	-1 (1)	-58 (-53)	-7 (-5)	-26 (-28)
Fractional Error (%)	62 (60)	20	88 (84)	9 (10)	70

Table 4: Summary of FEPS plume-rise scenario matched threshold comparison (SMOKE plume-rise scenario shown in parentheses when different) from July 3 to August 23, 2007 (top) and June 22 to August 27, 2008 (bottom). "Matched Threshold" refers to both model and observation values being removed from the analysis if either is below the threshold in combination with satellite statistics using rural sites only.

July 3 - Aug. 22, 2007

Species	**A24-hr PM2.5 (*μg/m³)***	**AOD**	**Tot. Col. CO (E+18 molec./cm²)**	**Trop. Col. NO_2 (E+15 molec./cm²)**
Source	**EPA AQS**	**MODIS**	**AIRS**	**OMI**
Threshold	***10***	***0.3***	***1.9***	***1.0***
Paired Points	555	150	356	599
Correlation (r)	0.4 (0.5)	0.0	0.3 (0.4)	0.2
Measured Mean	16.8	0.5	2.1	1.7
Mean Bias	5.9 (-0.1)	-0.3	-0.3 (-0.2)	-1.1
Mean Error	19.1 (12.1)	0.4	0.4	1.2
Normalized Mean Bias (%)	24 (-3)	-66 (-47)	-15 (-8)	-59 (-60)
Normalized Mean Error (%)	104 (70)	77 (84)	17 (19)	68
Fractional Bias (%)	-38 (-36)	-117 (-101)	-18 (-10)	-97 (-98)
Fractional Error (%)	80 (-10)	123 (115)	19	101 (102)

June 22 -Aug. 27, 2008

Species	**A24-hr PM2.5 (*μg/m³)***	**AOD**	**Tot. Col. CO (E+18 molec./cm²)**	**Trop. Col. NO_2 (E+15 molec./cm²)**
Source	**EPA AQS**	**MODIS**	**AIRS**	**OMI**
Threshold	***10***	***0.3***	***1.9***	***1.0***
Paired Points	872	260	521	755
Correlation (r)	0.4	0.1 (0.23	0.3 (0.2)	0.3
Measured Mean	15.9	0.5	2.1	1.6
Mean Bias	-6.5 (-5.6)	-0.4 (-0.3)	-0.3 (-0.2)	-0.9
Mean Error	9.0 (8.4)	0.4	0.3	1.1
Normalized Mean Bias (%)	-35 (-33)	-73 (60)	-11 (-8)	-54 (-57)
Normalized Mean Error (%)	56 (53)	77 (75)	12	66
Fractional Bias (%)	-66 (-57)	-125 (-105)	-12 (-9)	-90 (-93)
Fractional Error (%)	77 (71)	128 (113)	14 (13)	95 (97)

Table 5: Plume top height model comparisons with CALIOP for the FEPS plume-rise scenario (SMOKE plume-rise scenario shown in parentheses when different). Please note that some plumes contribute multiple paired points.

Year	**2007**		**2008**	
Vertical Reference	**AGL**	**AMSL**	**AGL**	**AMSL**
Paired Points	219 (218)	219 (218)	275 (281)	275 (281)
Correlation (*r*)	0 (0.2)	0.2 (0.4)	0.6 (0.5)	0.8
Measured Mean (km)	5.2 (5.1)	8.2 (8.0)	3.5	5.6
Mean Bias (km)	-1.4 (-1.5)	-3.1	-1.0 (-0.9)	-2.3 (-2.2)
Mean Error (km)	2.1 (1.9)	3.3 (3.2)	1.3 (1.2)	2.3 (2.2)
Normalized Mean Bias (%)	-3 (-10)	-34 (-35)	-16 (-10)	-39 (-35)
Normalized Mean Error (%)	52 (45)	38	43 (42)	40 (36)
Fractional Bias (%)	-28	-46	-32 (-26)	-52 (-46)
Fractional Error (%)	46 (45)	49 (48)	45 (42)	53 (48)

Table 6: PM2.5 National Ambient Air Quality Standards summary for both 2007 and 2008 fire periods analyzed per site per day for the FEPS plume-rise scenario (change due to SMOKE plume-rise scenario shown in parentheses).

24-hr NAAQS Threshold (35 ug/m3)						
Year	Monitors	Days	Matched Exceedances	Predictions Unmatched	Observations Unmatched	No Exceedances
2007	67	51	12	77 (-21)	10	3168 (+21)
2008	82	67	5 (-1)	74 (-20)	19 (+1)	5231 (+20)
		Totals:	17 (-1)	151 (-41)	29 (+1)	8399 (+41)
		Percent:	0.2%	1.8% (-0.5%)	0.3%	97.7% (+0.5%)
Annual NAAQS Threshold (12 ug/m3)						
Year	Monitors	Days	Matched Exceedances	Predictions Unmatched	Observations Unmatched	No Exceedances
2007	67	51	157 (+12)	206 (-25)	242 (-12)	5929 (+25)
2008	82	67	146 (+40)	393 (+34)	454 (-40)	9665 (-34)
		Totals:	303 (+52)	599 (+9)	696 (-50)	15594 (-9)
		Percent:	1.8% (+0.3%)	3.5%	4.0% (-0.3%)	90.7%

Fig. 1: Fire events with individual burn areas greater than 5000 acres during the analysis periods of 2007 (orange) and 2008 (red). Total fuel loading derived from the FCCS v1 is also shown for the AIRPACT-3 domain.

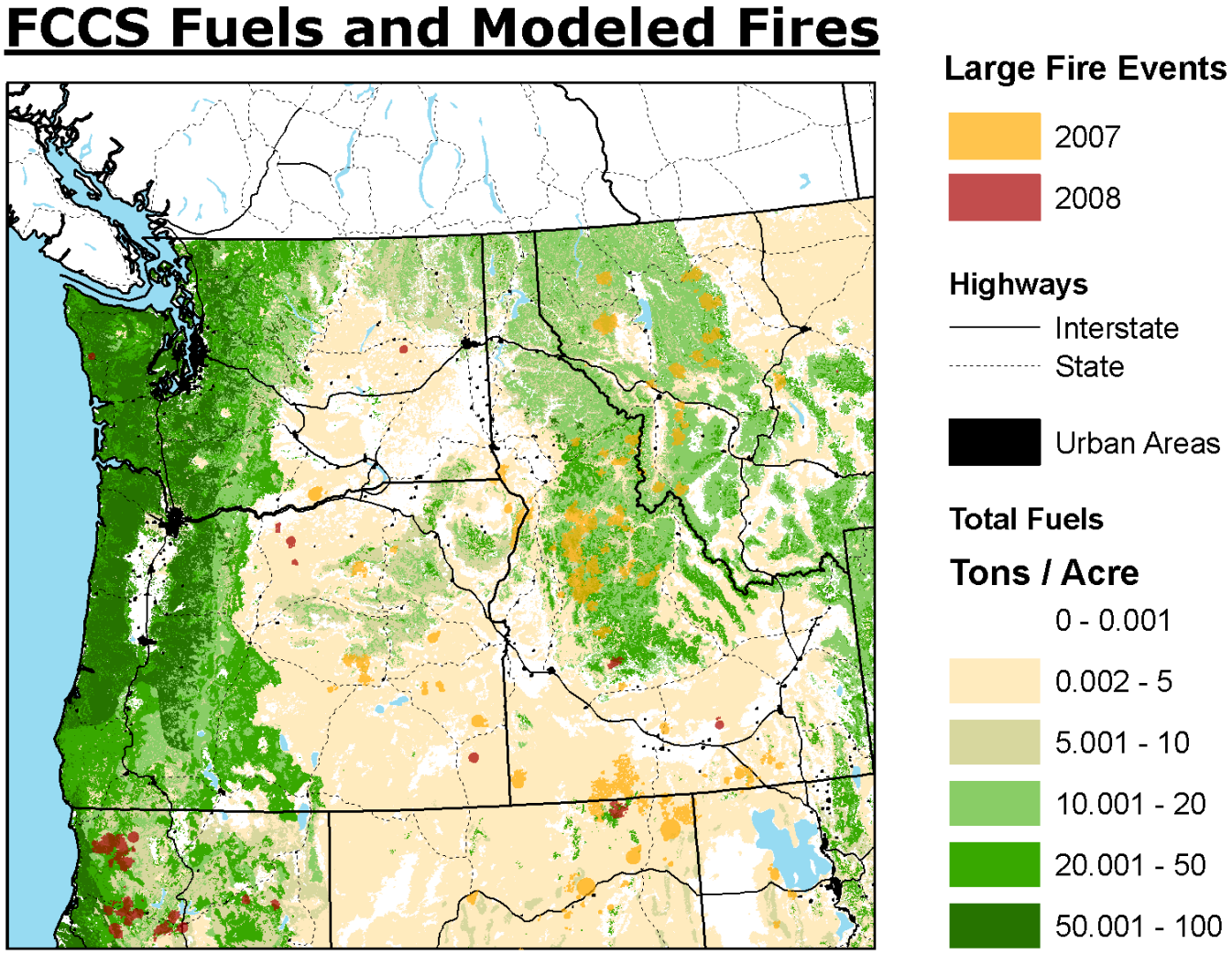

Fig. 2: Fire-related modeling pathways used in the AIRPACT-3 simulations.

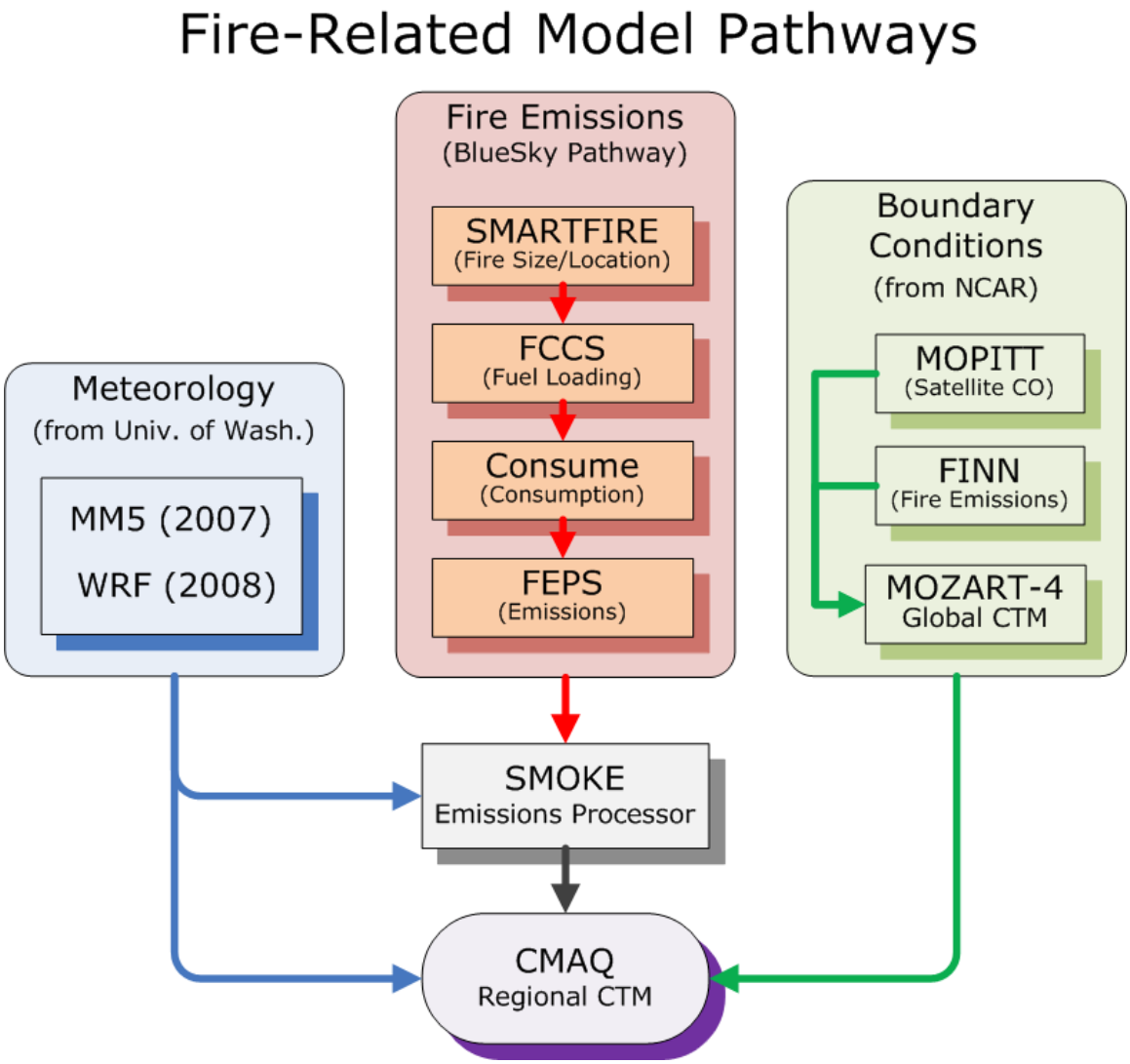

Fig. 3: AOD (left column), tropospheric NO2 columns (middle column), and total carbon monoxide columns (right column) for July 22, 2007 (~ 2 p.m. LST) with NASA EOS retrieval (top row), AIRPACT-3 with SMOKE plume rise (middle row), and differences (bottom row). Grey color indicates no or low-quality data from the satellite retrieval and exclusion from analysis. Values greater than the color scale maximum are shown as pink in the AIRPACT-3 and NASA EOS maps. Values outside the range of the difference color scales are shown as saturated blue/red.

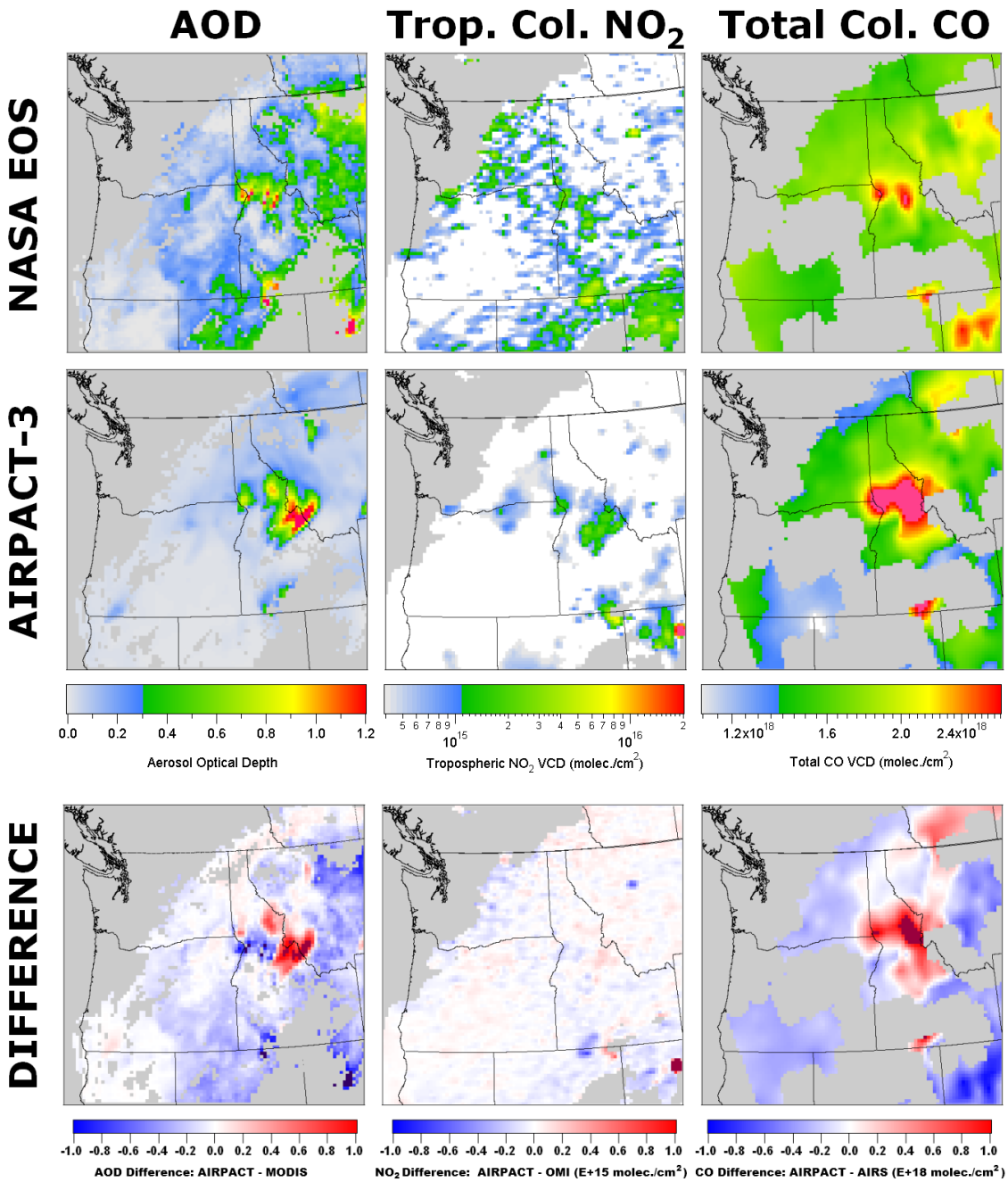

Fig. 4: AOD (left column), tropospheric NO_2 columns (middle column), and total carbon monoxide columns (right column) for August 12, 2007 (~ 2 p.m. LST) with NASA EOS retrieval (top row), AIRPACT-3 with SMOKE plume rise (middle row), and differences (bottom row). Grey color indicates no or low-quality data from the satellite retrieval and exclusion from analysis. Values greater than the color scale maximum are shown as pink in the AIRPACT-3 and NASA EOS maps. Values outside the range of the difference color scales are shown as saturated blue/red.

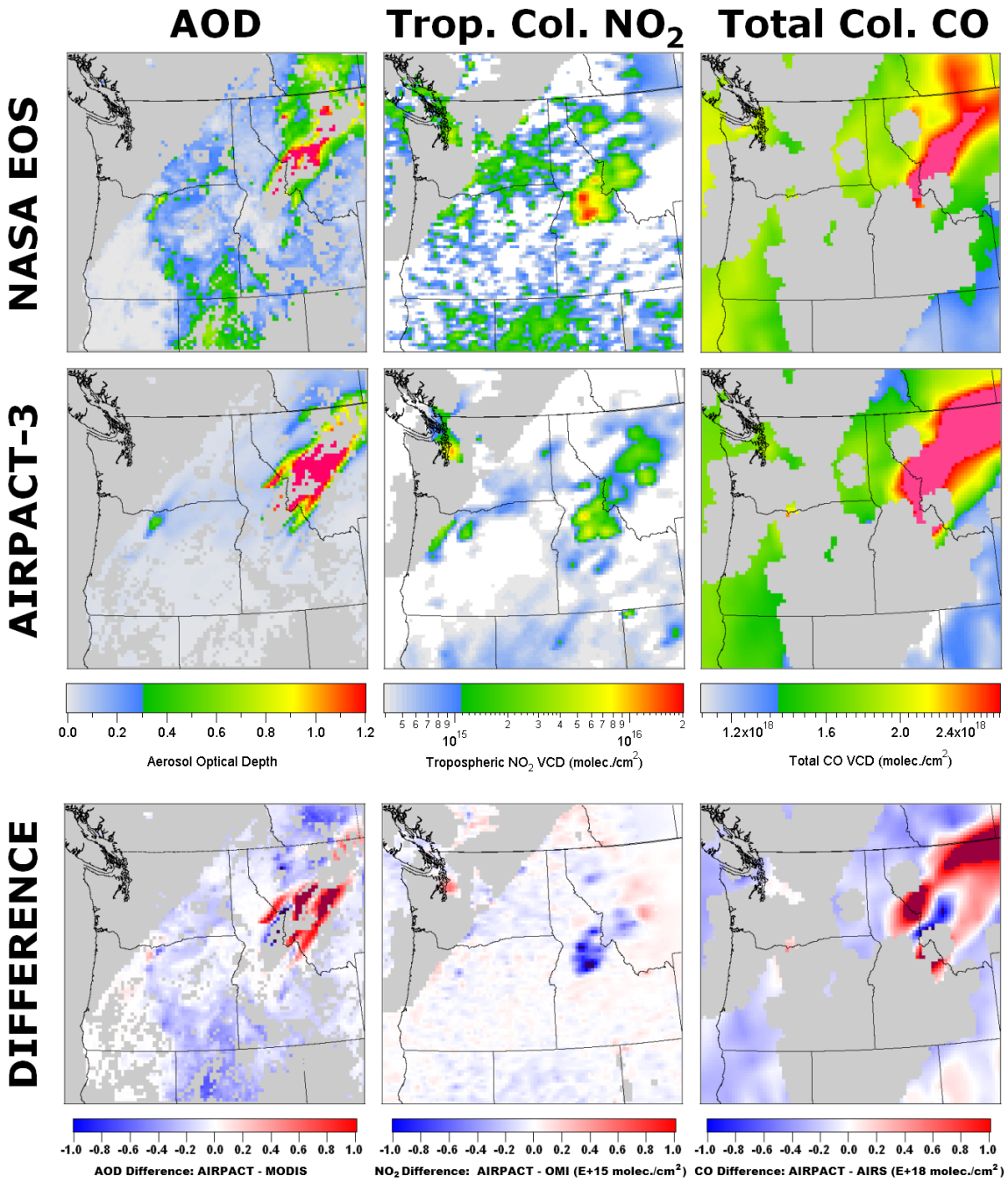

Fig. 5: AOD (left column), tropospheric NO_2 columns (middle column), and total carbon monoxide columns (right column) for June 29, 2008 (~ 2 p.m. LST) with NASA EOS retrieval (top row), AIRPACT-3 with SMOKE plume rise (middle row), and differences (bottom row). Grey color indicates no or low-quality data from the satellite retrieval and exclusion from analysis. Values greater than the color scale maximum are shown as pink in the AIRPACT-3 and NASA EOS maps. Values outside the range of the difference color scales are shown as saturated blue/red.

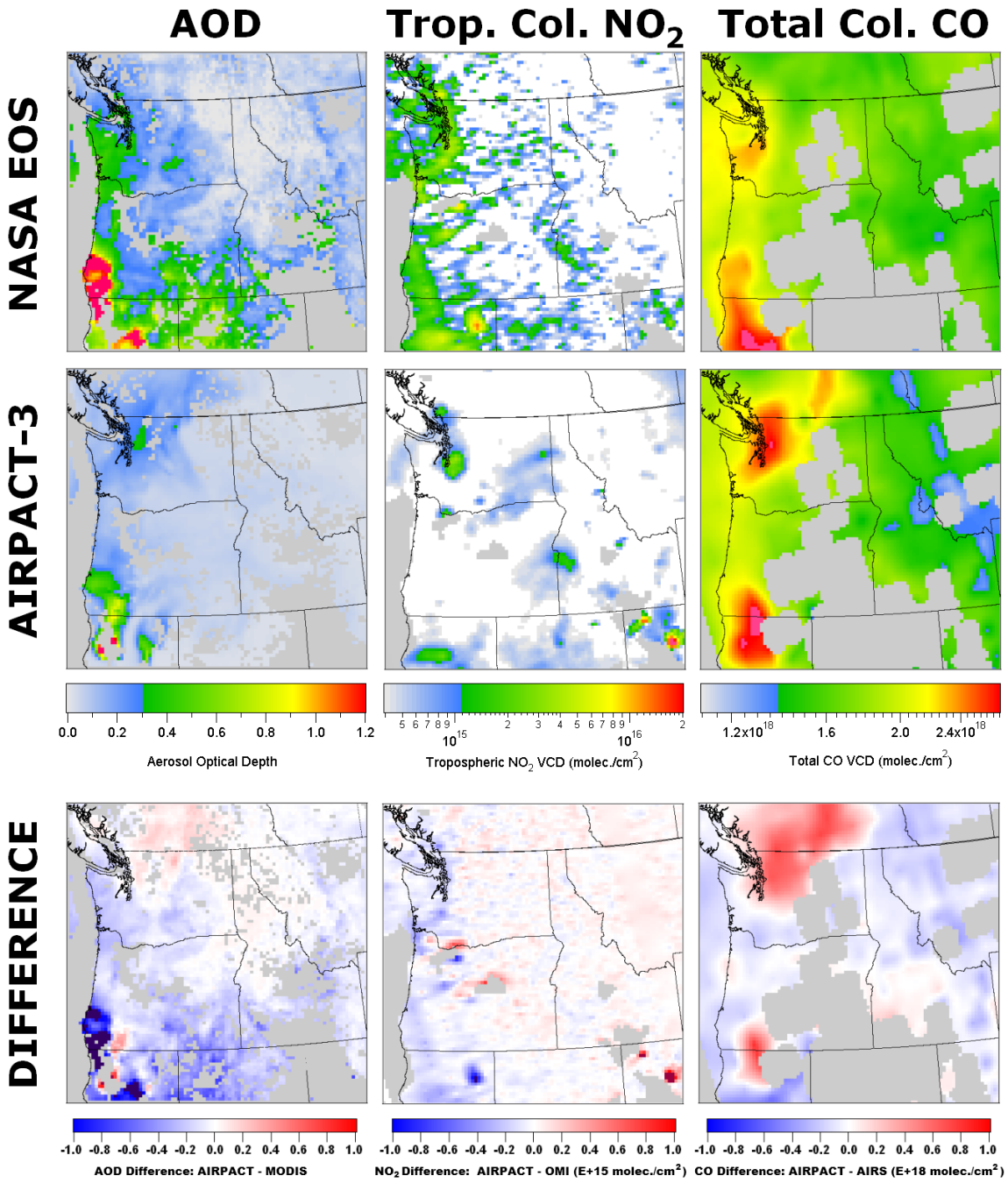

Fig. 6: AOD (left column), tropospheric NO_2 columns (middle column), and total carbon monoxide columns (right column) for July 20, 2008 (~ 2 p.m. LST) with NASA EOS retrieval (top row), AIRPACT-3 with SMOKE plume rise (middle row), and differences (bottom row). Grey color indicates no or low-quality data from the satellite retrieval and exclusion from analysis. Values greater than the color scale maximum are shown as pink in the AIRPACT-3 and NASA EOS maps. Values outside the range of the difference color scales are shown as saturated blue/red. Mt Bachelor is shown as a black triangle near central Oregon.

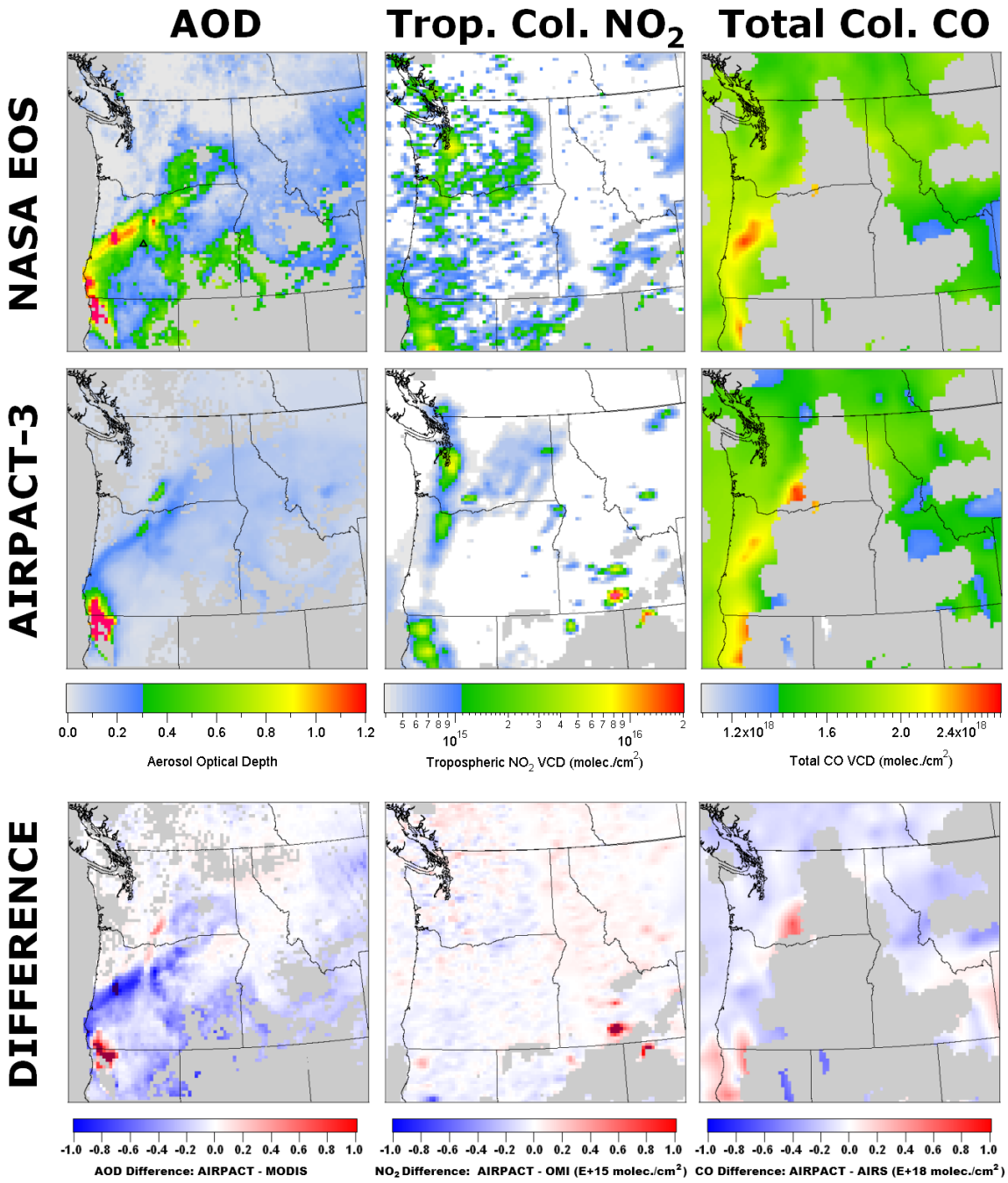

Fig. 7: AIRPACT-3 vs. CALIOP plume top heights for 2007 (red) and 2008 (blue) when CALIPSO passed over the Idaho and California wildfires, respectively (~ 2 p.m. LST). Plume top heights above sea level (left) and above ground level (right) are shown for both the FEPS plume rise (open circle) and SMOKE plume rise (solid dot) scenarios. Note that plume top heights are only shown for locations where both CALIOP and AIRPACT-3 showed an aerosol plume.

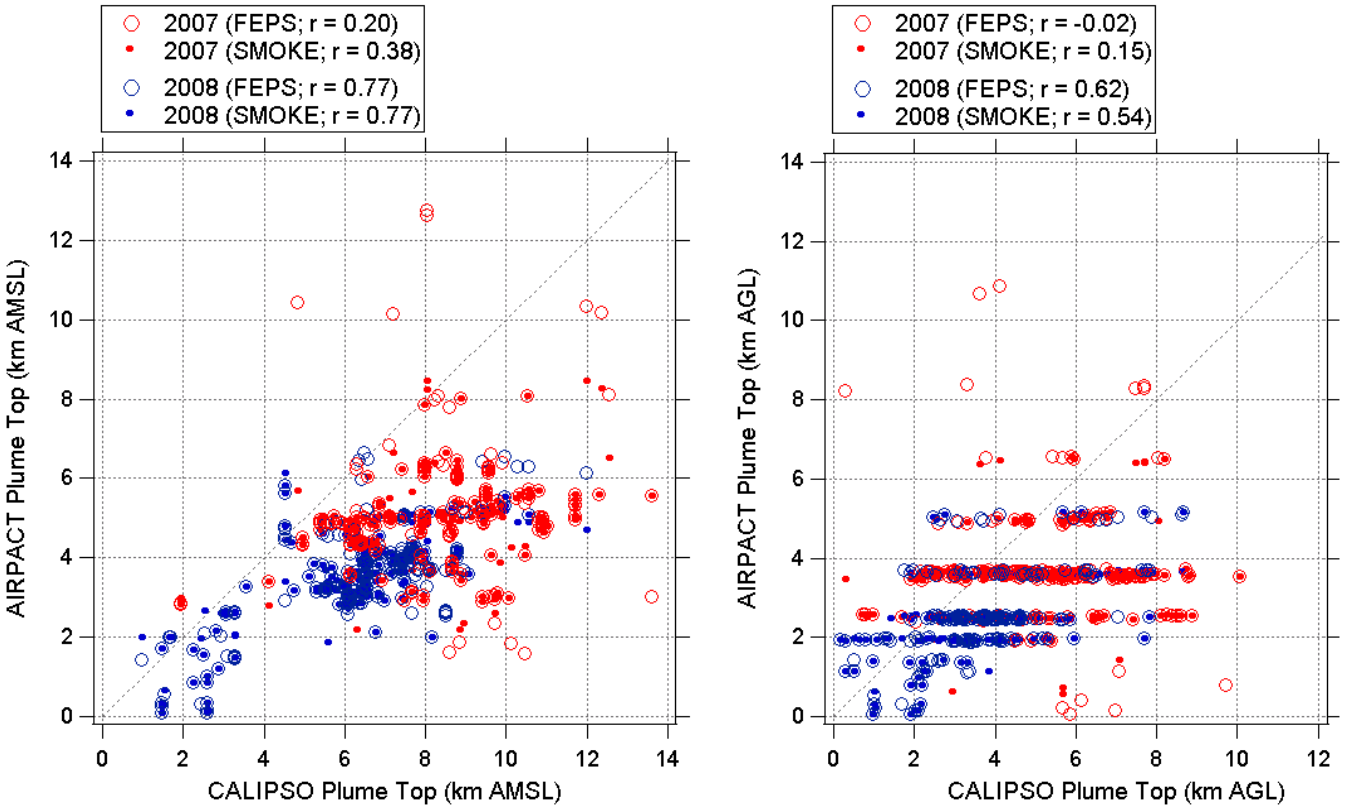

Fig. 8: July 3 to August 22, 2007 (top) Daily 24-hr average $PM_{2.5}$ averaged across 67 sites (a) and Max Daily 8-hr average ozone averaged across 10 sites (b); June 22 to August 27, 2008 (bottom) Daily 24-hr average PM2.5 averaged across 82 sites (c) and Max Daily 8-hr average ozone averaged across 18 sites (d) from. Model simulations are shown in red with squares (FEPS plume rise) and orange dotted (SMOKE plume rise) while observations are shown in dotted blue with diamonds.

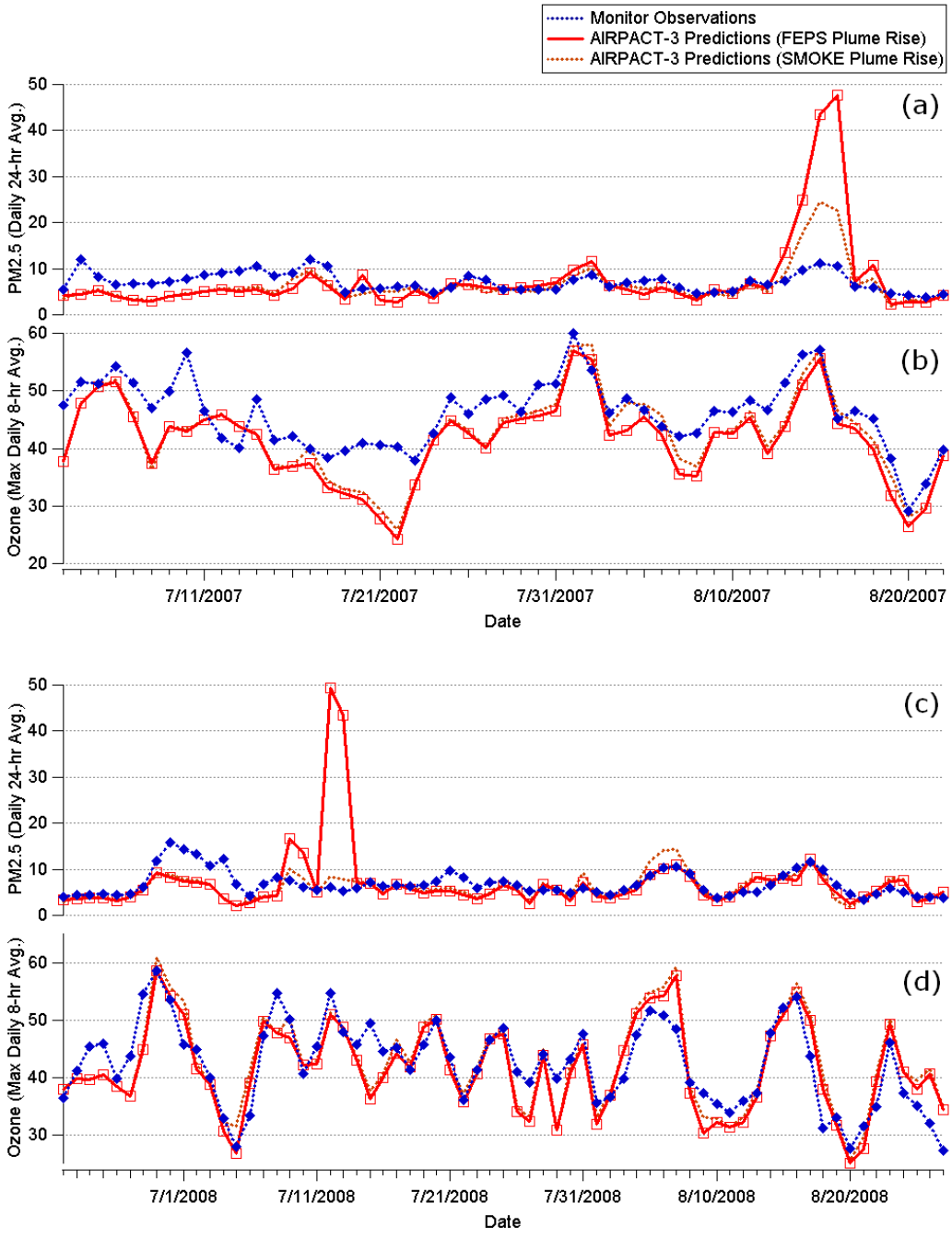

Fig. 9: Particulate Matter (top), carbon monoxide (middle), and ozone (bottom) at Mt. Bachelor Observatory for July 12 to August 21, 2008. AIRPACT-3 model simulations are shown in red (FEPS plume rise) and orange (SMOKE plume rise), MOZART-4 model simulations are shown in black, and observations are shown in dotted blue. Note that aerosols for AIRPACT-3 are reported as $PM_{2.5}$ and observed aerosols are sub-micron aerosols converted from scattering observations using the method described in Wigder et al., (2013).